NASA TECHNICAL NOTE

NASA TN D-4576

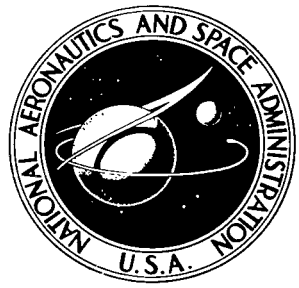

THE DYNAMIC CHARACTERISTICS OF SATELLITES HAVING LONG ELASTIC MEMBERS

by Harold P. Frisch

Goddard Space Flight Center
Greenbelt, Md.

NATIONAL AERONAUTICS AND SPACE ADMINISTRATION • WASHINGTON, D. C. • AUGUST 1968

THE DYNAMIC CHARACTERISTICS OF SATELLITES HAVING LONG ELASTIC MEMBERS

By Harold P. Frisch

Goddard Space Flight Center
Greenbelt, Md.

NATIONAL AERONAUTICS AND SPACE ADMINISTRATION

For sale by the Clearinghouse for Federal Scientific and Technical Information
Springfield, Virginia 22151 – CFSTI price $3.00

ABSTRACT

Many satellites, such as ATS-A, ATS-D, DODGE, RAE, etc., have clamped to the surface of their central body long elastic members which when set into vibratory motion can significantly influence the motion of the central body. If such a satellite is reasonably symmetrical, we can predict its dynamic characteristics by modeling the entire satellite as a symmetric double-beam system; that is, by a rigid symmetric central body having clamped to its surface two long, diametrically opposed uniform elastic beams with tip weights possessing identical physical and geometrical properties. In this paper, dimensionless equations which define the natural modes and frequencies of such a satellite system are derived and solved. The solutions are outlined in graphical form and then used to solve the equations that describe the elastic response of the satellite to an arbitrary periodic forcing function. The results in both graphical and analytical form make it possible to predict with slide-rule accuracy the natural frequencies of any satellite that can be modeled as a symmetric double-beam system. The dynamic response equations have been applied to a particular problem associated with ATS-D. It is shown that if the ATS-D microthruster were operated at any frequency, including the system resonants, the viscoelastic damping of the elastic beams would be sufficient to prevent the resonant-oscillation amplitudes from exceeding the elastic limits of the attached appendages.

CONTENTS

THE DYNAMIC CHARACTERISTICS OF SATELLITES HAVING LONG ELASTIC MEMBERS

by
Harold P. Frisch
Goddard Space Flight Center

INTRODUCTION

The design and computer simulation of an active control system for a satellite having long elastic members (booms) requires knowledge of each elastic mode of vibration that can be excited, and its associated natural frequency. This is essential for system design, and helps to develop and verify the computer simulation of the entire coupled dynamic system.

To predict with accuracy each vibration mode and resonant frequency, we must account for the geometric configuration of the satellite system; the mass, size, and rotational inertia of the rigid satellite body; and the elastic properties of the appendages. Frequently the geometrical configuration permits describing the satellite by a symmetric double-beam model, that is: two diametrically opposed uniform elastic beams with tip weights, attached to a rigid central body having mass, finite size, and rotational inertia (Figure 1). It is this type of satellite system that will be extensively discussed in this paper.

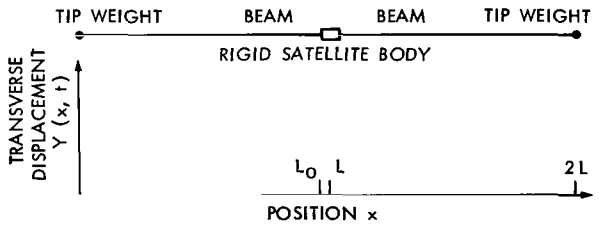

Figure 1—Symmetric double-beam satellite system.

The equations developed in dimensionless form and the results given provide sufficient information to permit computing, with slide-rule accuracy, the natural frequencies of each of the pertinent modes of vibration for any such satellite. By comparing the natural frequencies with those resulting from the limiting cases of zero or infinite satellite body weight, rotational inertia, or tip weight, it is possible to justify further simplifications in a detailed computer simulation of the entire satellite control system.

Such a system (as shown in Figure 1) is symmetrical with respect to a plane passing through its center of mass. Therefore, the natural modes of vibration can be separated into two groups: those that are symmetric about the axis of symmetry, and those that are antisymmetric about the axis of symmetry relative to the point on the axis that is coincident with the system's center of mass. The axis of symmetry is defined as that which is normal to the undeflected shape of the

system, passing through the center of mass and in the plane of vibration. This symmetry permits one to derive the two frequency equations and the mode shapes of the entire system by simply solving the vibration equation over the elastic portion of one beam twice: once with the boundary conditions associated with the symmetric modes of vibration, and again with the boundary conditions associated with the antisymmetric modes of vibration.

The derived modes form a set of orthogonal functions; these can be used to obtain a series solution to the equation describing the vibrational motion of each point of the system.

To obtain the solution the applied force distribution is decomposed into an equivalent force system. That is:

1. A force distribution, symmetric about the system's axis of symmetry, which excites only the symmetric modes of vibration, and

2. A force distribution, antisymmetric about the system's axis of symmetry, which excites only the antisymmetric modes of vibration.

It follows from the principle of superposition that the system's dynamic response to the equivalent force system is identical with its dynamic response to the actual force distribution.

The derived equations, to illustrate these results, are used to solve a particular problem associated with ATS-D. They are specialized so as to describe the response of the satellite system to a microthruster of periodic intensity located at the point where one of the booms is attached to the rigid central body. It is shown that the viscoelastic damping of the boom material itself is enough to prevent the peak bending moment at every point of the system from exceeding the critical buckling moment of the boom itself, even if the thruster excites a system resonant frequency.

1. BASIC THEORY

The equations and results presented here can be applied to any satellite that can be modeled as the symmetric double-beam system shown in Figure 1. This is an elastic system, which has two identical diametrically opposed uniform elastic beams with tip weights, clamped to the surface of a rigid central body. The central body is assumed to be perfectly rigid and have finite size, mass, and rotational inertia. Thus the elastic system under study is treated as one having discontinuities in mass and stiffness along its length.

The present analysis first derives the orthogonal functions that define the normal modes of vibration and the corresponding frequency equations, in a form that may be readily applied to any similar system. These equations are then used to analytically solve the damped forced-vibration equation. The partial differential equation for the damped vibrational motion of every point along the systems length, when it is excited by a known force distribution, is

$$\frac{\partial^2}{\partial x^2} EI(x) \frac{\partial^2 Y(x, t)}{\partial x^2} + \rho(x) \frac{\partial^2 Y(x, t)}{\partial t^2} + \beta(x) \frac{\partial Y(x, t)}{\partial t} = F(x, t) , \tag{1.1}$$

where

x = position coordinate measured positive from the boom tip, ft (Figure 1)

t = time, sec

$Y(x, t)$ = transverse displacement at (x, t), ft

$F(x, t)$ = external force distribution at (x, t), lb ft^{-1}

$\rho(x)$ = mass distribution at x, slugs ft^{-1}

$EI(x)$ = bending stiffness at x, lb ft^2

$\beta(x)$ = viscous damping coefficient at x, lb sec ft^{-2}.*

When the viscous damping coefficient $\beta(x)$ is proportional to the mass distribution $\rho(x)$ equation 1.1 can be solved by separation of variables; the resulting solution is of the form

$$Y(x, t) = \sum_{n=1}^{\infty} a_n(t) y_n(x) , \tag{1.2}$$

where

$y_n(x)$ is the nth normalized mode of the undamped unforced equations of motion of the entire system, and

$a_n(t)$ is the time-dependent generalized displacement coordinate associated with the nth mode, feet.

These mode shapes $y_n(x)$ that are to be used in Equation 1.2 must be derived from the equation

$$\frac{\partial^2}{\partial x^2} EI(x) \frac{\partial^2 Y(x, t)}{\partial x^2} + \rho(x) \frac{\partial^2 Y(x, t)}{\partial t^2} = 0 \tag{1.3}$$

and must satisfy the time-independent boundary conditions of the system.

Because, when the system vibrates in any one of its normal modes of vibration the deflection of every point of the system varies harmonically in time, the solution to Equation 1.3 is of the form

$$Y(x, t) = y(x) e^{i\omega t} , \tag{1.4}$$

where $y(x)$ defines the shape of the normal mode and ω is its frequency of vibration (radians sec^{-1}).

*For a complete symbol list, see Appendix A.

Directly substituting Equation 1.4 in Equation 1.3 gives the differential equation

$$\frac{d^2}{dx^2} EI(x) \frac{d^2 y(x)}{dx^2} - \rho(x) \omega^2 y(x) = 0 \tag{1.5}$$

Equation 1.5, along with its time-independent boundary conditions, defines an eigenvalue problem. The eigenvalues, which are the solutions to the characteristic (frequency) equation of the problem, define the natural frequencies of the system, and the eigenvectors associated with each of the eigenvalues define the orthogonal modes of the system.

Since Equation 1.5 has parametric discontinuities along its length which cannot be assumed negligible a geometric construction must be used to develop solutions to this equation.

Reference 1 states that the mode shapes that are assumed to satisfy the equation

$$\frac{d^2}{dx^2} EI(x) \frac{d^2 y_n(x)}{dx^2} - \rho(x) \omega_n^2 y_n(x) = 0 \tag{1.6}$$

must satisfy two basic criteria: they must impose as little constraint as possible on the motion of the system, and they must satisfy the kinematic boundary conditions. It is also extremely useful but not essential that the constructed modes be orthogonal.

The actual mode shapes $y_n(x)$, defined over the entire system length, that satisfy Equation 1.6 are obtained as follows:

1. Note that the complete set of natural modes of vibration can be divided into two groups:
   a. Those symmetric about the system's axis of symmetry: "symmetric modes of vibration."
   b. Those antisymmetric about the system's axis of symmetry relative to the point coincident with the system's center of mass: "antisymmetric modes of vibration."
2. Let

   EI = bending stiffness, uniform along length of elastic beam, lb ft^2,

   ρ = mass distribution, uniform along length of elastic beam, slugs ft^{-1},

then solve the eigenvalue problem defined by the equation

$$EI \frac{d^4 y(x)}{dx^4} - \rho\omega^2 y(x) = 0 \tag{1.7}$$

over the elastic portion of half of the system; that is, over the length of one beam twice, as follows:

a. Use the boundary conditions that define the effect of the central body's mass on the beam at its point of attachment, and the effect of the tip weight on the beam at its point of attachment, when the system is vibrating in one of the symmetric modes of vibration.

b. Use the boundary conditions that define the effect of the central body's size and rotational inertia on the beam at its point of attachment, and the effect of the tip weight on the beam at its point of attachment, when the system is vibrating in one of the antisymmetric modes of vibration.

3. Reflect about the system's axis of symmetry each derived eigenvector of Equation 1.7, symmetrically or antisymmetrically as dictated by the boundary conditions. The two points analogous to the points at which the beams are attached to the central body will then be displaced by a distance 2R, the length of the central body, from each other. Connecting these two points with a linear segment generates a function that is definable at every point along the system's length.

This function satisfies Equation 1.6 at every point along the flexible portion of the system; it satisfies all boundary conditions and accounts for the length and rigidity of the satellite body. Furthermore, since the eigenvectors of Equation 1.7 are orthogonal and the satellite length is small compared to the system length, the symmetric and antisymmetric modes will form two sets of orthogonal functions. It is easily shown that these two sets are mutually orthogonal by noting that the integral of the product of an odd and an even function over symmetric limits is zero.

Note that each mode shape as constructed is not unique but defined only up to a multiplicative constant. The mode shapes, however, can be made unique by requiring that the orthonormality condition

$$\int_0^{2L} \rho(x)\, y_n(x)\, y_m(x)\, dx = M_T\, \delta_{n,m} \tag{1.8}$$

be satisfied for all integers n and m, where

M_T = total mass of system, slugs,

2L = total length of system, ft,

$$\delta_{n,m} = \begin{cases} 0 & \text{if } n \neq m, \text{ the Kronecker delta function} \\ 1 & \text{if } n = m. \end{cases}$$

2. NATURAL MODES AND FREQUENCIES

As previously mentioned, the natural modes and frequencies of the system are constructed from the solutions to Equation 1.7 along with the appropriate boundary conditions that define the symmetric and antisymmetric modes.

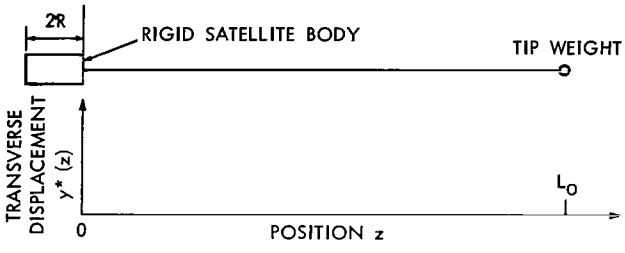

Figure 2—Coordinate system used to derive frequency equations.

In order to avoid notational difficulties it is convenient to define the parameter z over the elastic portion of half the system, as shown in Figure 2. Since z is linearly related to x, Equation 1.7 can be rewritten as

$$EI \frac{d^4 y^*(z)}{dz^4} - \rho\omega^2 y^*(z) = 0 \qquad (2.1)$$

and the boundary conditions defined at the points $z = 0$ and $z = L_0 = L - R$, L_0 being the length of one beam. This equation has the general solution

$$y^*(z) = C_1 \cosh \lambda z + C_2 \sinh \lambda z + C_3 \cos \lambda z + C_4 \sin \lambda z \ , \qquad (2.2)$$

where

$$\lambda^4 = \frac{\rho\omega^2}{EI} \qquad (2.3)$$

and C_1, C_2, C_3, C_4 are constants of integration.

The actual values of λ to be used in Equations 2.2 and 2.3 are the solutions to the frequency equations of the system, which are derivable from the equations defining the boundary conditions.

The boundary conditions for the two cases mentioned are:

Symmetric modes of vibration:

$$\left.\frac{dy^*(z)}{dz}\right|_{z=0} = 0 \ ,$$

$$\left. - EI \frac{d^3 y^*(z)}{dz^3} + \frac{W_s}{2g} \omega^2 y^*(z) \right|_{z=0} = 0 \ ,$$

$$\left. EI \frac{d^2 y^*(z)}{dz^2} \right|_{z=L_0} = 0 \ ,$$

$$\left. EI \frac{d^3 y^*(z)}{dz^3} + \frac{W_T}{g} \omega^2 y^*(z) \right|_{z=L_0} = 0 \ , \qquad (2.4)$$

Antisymmetric modes of vibration:

$$\left.\frac{dy^*(z)}{dz} - \frac{1}{R}\, y^*(z)\right|_{z=0} = 0 ,$$

$$\left. - EI\, R\, \frac{d^3 y^*(z)}{dz^3} + EI\, \frac{d^2 y^*(z)}{dz^2} + \frac{I_s}{2R}\, \omega^2\, y^*(z)\right|_{z=0} = 0 ,$$

$$\left. EI\, \frac{d^2 y^*(z)}{dz^2}\right|_{z=L_0} = 0 ,$$

$$\left. EI\, \frac{d^3 y^*(z)}{dz^3} + \frac{W_T}{g}\, \omega^2\, y^*(z)\right|_{z=L_0} = 0 , \qquad (2.5)$$

where

W_T = tip weight, lb,

W_s = weight of rigid satellite body (without beams and tip weights), lb,

I_s = mass moment of inertia of rigid satellite body (without beams and tip weights) about the axis through the center of mass and normal to the plane of vibration, slugs ft^2,

g = acceleration of gravity, ft sec^{-2},

$L_0 = L - R$ = length of one beam, ft,

$2R$ = length of satellite body, ft,

$2L$ = length of entire system, ft.

The frequency equation associated with each case is derived by substituting the general solution (Equation 2.2) in the four equations defining the boundary conditions. This yields four homogeneous equations in the four unknowns, C_1, C_2, C_3, C_4, for each case. It follows that for a nontrivial solution to exist, the determinant of the coefficients of C_1, C_2, C_3, C_4 must be identically equal to zero. The evaluation of this determinant yields a transcendental equation in λ—commonly referred to as the "frequency equation." Thus:

Frequency equation for symmetric modes of vibration:

A direct substitution of the general solution, Equation 2.2, in the four boundary conditions, Equations 2.4, yields:

$$C_2 + C_4 = 0$$

$$C_1 \cosh \lambda L_0 + C_2 \sinh \lambda L_0 - C_3 \cos \lambda L_0 - C_4 \sin \lambda L_0 = 0$$

$$- EI\lambda^3 (C_2 - C_4) + \frac{W_s}{2g} \omega^2 (C_1 + C_3) = 0$$

$$EI\lambda^3 (C_1 \sinh \lambda L_0 + C_2 \cosh \lambda L_0 + C_3 \sin \lambda L_0 - C_4 \cos \lambda L_0)$$

$$+ \frac{W_T}{g} \omega^2 (C_1 \cosh \lambda L_0 + C_2 \sinh \lambda L_0 + C_3 \cos \lambda L_0 + C_4 \sin \lambda L_0) = 0. \qquad (2.6)$$

For a non-trivial solution to exist, the determinant of the coefficients must be equal to zero; that is

$$\begin{vmatrix} q_{11} & q_{12} & q_{13} & q_{14} \\ q_{21} & q_{22} & q_{23} & q_{24} \\ q_{31} & q_{32} & q_{33} & q_{34} \\ q_{41} & q_{42} & q_{43} & q_{44} \end{vmatrix} = 0 , \qquad (2.7)$$

where

$$q_{11} = 0 \qquad q_{21} = \cosh \lambda L_0$$

$$q_{12} = 1 \qquad q_{22} = \sinh \lambda L_0$$

$$q_{13} = 0 \qquad q_{23} = - \cos \lambda L_0$$

$$q_{14} = 1 \qquad q_{24} = - \sin \lambda L_0$$

$$q_{31} = \frac{W_s}{2W_B} \lambda L_0 \qquad q_{41} = \sinh \lambda L_0 + \frac{W_T}{W_B} \lambda L_0 \cosh \lambda L_0$$

$$q_{32} = - 1 \qquad q_{42} = \cosh \lambda L_0 + \frac{W_T}{W_B} \lambda L_0 \sinh \lambda L_0$$

$$q_{33} = \frac{W_s}{2W_B} \lambda L_0 \qquad q_{43} = \sin \lambda L_0 + \frac{W_T}{W_B} \lambda L_0 \cos \lambda L_0$$

$$q_{34} = 1 \qquad q_{44} = - \cos \lambda L_0 + \frac{W_T}{W_B} \lambda L_0 \sin \lambda L_0$$

$$W_B = \rho g L_0 = \text{weight of one beam, lb ,}$$

$$\lambda^4 = \frac{\rho \omega^2}{EI} . \qquad (2.8)$$

Directly substituting Equations 2.8 in Equation 2.7 gives the following:

$$\frac{W_T}{W_B} = -\frac{\tanh \lambda L_0 + \tan \lambda L_0 + \frac{W_s}{2W_B} \lambda L_0 \left(1 + \sec \lambda L_0 \operatorname{sech} \lambda L_0\right)}{2\lambda L_0 - \frac{W_s}{2W_B} (\lambda L_0)^2 \left(\tan \lambda L_0 - \tanh \lambda L_0\right)} . \tag{2.9}$$

This is the frequency equation for the beam of length L_0 having the prescribed boundary conditions. Furthermore, because of the symmetry of the system, it is also the frequency equation for the symmetric modes of the entire system.

Frequency equation for antisymmetric modes of vibration:

A direct substitution of the general solution, Equation 2.2, in the four boundary conditions, Equations 2.5, yields:

$$\lambda \left(C_2 + C_4\right) - \frac{1}{R} \left(C_1 + C_3\right) = 0$$

$$C_1 \cosh \lambda L_0 + C_2 \sinh \lambda L_0 - C_3 \cos \lambda L_0 - C_4 \sin \lambda L_0 = 0$$

$$-EIR \lambda^3 \left(C_2 - C_4\right) + EI\lambda^2 \left(C_1 - C_3\right) + \frac{I_s}{2R} \omega^2 \left(C_1 + C_3\right) = 0$$

$$EI\lambda^3 \left(C_1 \sinh \lambda L_0 + C_2 \cosh \lambda L_0 + C_3 \sin \lambda L_0 - C_4 \cos \lambda L_0\right)$$

$$+ \frac{W_T}{g} \omega^2 \left(C_1 \cosh \lambda L_0 + C_2 \sinh \lambda L_0 + C_3 \cos \lambda L_0 + C_4 \sin \lambda L_0\right) = 0 . \tag{2.10}$$

For a non-trivial solution to exist, the determinant of the coefficients must be equal to zero; that is:

$$\begin{vmatrix} q_{11} & q_{12} & q_{13} & q_{14} \\ q_{21} & q_{22} & q_{23} & q_{24} \\ q_{31} & q_{32} & q_{33} & q_{34} \\ q_{41} & q_{42} & q_{43} & q_{44} \end{vmatrix} = 0 \tag{2.11}$$

where

$$q_{11} = -\frac{1}{R^*} \qquad q_{21} = \cosh \lambda L_0$$

$$q_{12} = \lambda L_0 \qquad q_{22} = \sinh \lambda L_0$$

$$q_{13} = -\frac{1}{R^*} \qquad q_{23} = -\cos \lambda L_0$$

$$q_{14} = \lambda L_0 \qquad q_{24} = -\sin \lambda L_0$$

$$q_{31} = \frac{1}{R^*} + \frac{W_s^*}{2W_B} (\lambda L_0)^2$$

$$q_{32} = -\lambda L_0$$

$$q_{33} = -\frac{1}{R^*} + \frac{W_s^*}{2W_B} (\lambda L_0)^2$$

$$q_{34} = +\lambda L_0$$

$$q_{41} = \sinh \lambda L_0 + \frac{W_T}{W_B} \lambda L_0 \cosh \lambda L_0$$

$$q_{42} = \cosh \lambda L_0 + \frac{W_T}{W_B} \lambda L_0 \sinh \lambda L_0$$

$$q_{43} = \sin \lambda L_0 + \frac{W_T}{W_B} \lambda L_0 \cos \lambda L_0$$

$$q_{44} = -\cos \lambda L_0 + \frac{W_T}{W_B} \lambda L_0 \sin \lambda L_0$$

$W_B = \rho g L_0$ = weight of one beam, lb ,

$W_s^* = \frac{I_s g}{R^2}$ = effective inertia weight of rigid satellite body, lb ,

$R^* = \frac{R}{L_0}$ ▫ normalized satellite radius . (2.12)

Directly substituting Equations 2.12 in Equation 2.11 gives the following:

$$\frac{W_T}{W_B} = \frac{\left\{\tanh \lambda L_0 - \tan \lambda L_0 - 2\lambda L_0 R^* \tan \lambda L_0 \tanh \lambda L_0 - (\lambda L_0 R^*)^2 (\tanh \lambda L_0 + \tan \lambda L_0) - \frac{W_s^*}{2W_B} R^{*2} (\lambda L_0)^3 (1 + \sec \lambda L_0 \operatorname{sech} \lambda L_0)\right\}}{\left\{\lambda L_0 \left[2 \tan \lambda L_0 \tanh \lambda L_0 + 2R^* \lambda L_0 (\tanh \lambda L_0 + \tan \lambda L_0) + 2(R^* \lambda L_0)^2 + \frac{W_s^*}{2W_B} R^{*2} (\lambda L_0)^3 (\tanh \lambda L_0 - \tan \lambda L_0)\right]\right\}} \tag{2.13}$$

Let

I_B = mass moment of inertia of a beam of length $2L_0$ about an axis normal to the length and passing through its centroid, slugs ft^2.

Then

$$I_B = \frac{2}{3} \rho L_0^3 . \tag{2.14}$$

This expression can be used to rewrite Equation 2.13 in terms of the inertia ratio I_s/I_B. That is, by substituting

$$\frac{W_s^*}{W_B} = \frac{I_s g}{\rho g L_0 R^2} = \frac{I_s}{\rho L_0^3 R^{*2}} = \frac{2I_s}{3I_B R^{*2}} \tag{2.15}$$

in Equation 2.13:

$$\frac{W_T}{W_B} = \frac{\left\{\tanh \lambda L_0 - \tan \lambda L_0 - 2\lambda L_0 R^* \tan \lambda L_0 \tanh \lambda L_0 - (\lambda L_0 R^*)^2 (\tanh \lambda L_0 + \tan \lambda L_0) - \frac{I_s}{3I_B} (\lambda L_0)^3 (1 + \sec \lambda L_0 \operatorname{sech} \lambda L_0)\right\}}{\left\{\lambda L_0 \left[2 \tan \lambda L_0 \tanh \lambda L_0 + 2\lambda L_0 R^* (\tanh \lambda L_0 + \tan \lambda L_0) + 2(\lambda L_0 R^*)^2 + \frac{I_s}{3I_B} (\lambda L_0)^3 (\tanh \lambda L_0 - \tan \lambda L_0)\right]\right\}} . \tag{2.16}$$

This is the frequency equation for the beam of length L_0 having the prescribed boundary conditions. Furthermore, because of the symmetry of the system, it is also the frequency equation for the antisymmetric modes of the entire system.

Equations 2.9 and 2.16 are transcendental equations that cannot be readily simplified except for extreme values of the dimensionless ratios included. For any particular set of parameters, however, the equations can be solved accurately by numerical techniques.

It is convenient to put those values of λL_0 that satisfy Equation 2.9 and 2.16, in a particular order. That is, let:

$(\lambda L_0)_{2n-1}$ = the nth value of λL_0 (in increasing order of magnitude) that satisfies the frequency equation for the symmetric modes of vibration, Equation 2.9,

$(\lambda L_0)_{2n}$ = the nth value of λL_0 (in increasing order of magnitude) that satisfies the frequency equation for the antisymmetric modes of vibration, Equation 2.16.

Thus, from Equation 2.3, the mth natural frequency of the system is given by

$$\omega_m = \lambda_m^2 \sqrt{\frac{EI}{\rho}} , \tag{2.17}$$

where it is understood that

$$\lambda_m = \frac{(\lambda L_0)_m}{L_0} \tag{2.18}$$

Associated with each eigenvalue λ_m there exists an eigenvector $y_m^*(z)$ that satisfies the differential equation

$$\frac{d^4 y_m^*(z)}{dz^4} - \lambda_m^4 y_m^*(z) = 0 \tag{2.19}$$

and the four boundary conditions given by Equations 2.4 or 2.5. This function $y_m^*(z)$, along with the orthonormality condition, Equation 1.8, is used to construct $y_m(x)$, the mth natural mode of the entire system.

The equation defining $y_m^*(z)$ is derived as follows:

m odd; symmetric modes:

Let C_{1m}, C_{2m}, C_{3m}, C_{4m} be the constants of integration associated with the mth natural frequency ω_m. Directly substituting λ_m into the first three of Equations 2.6 and solving for the constants leads to:

$$C_{2m} = -C_{4m} ,$$

$$C_{1m} \cosh \lambda_m L_0 + C_{2m} (\sinh \lambda_m L_0 + \sin \lambda_m L_0) = C_{3m} \cos \lambda_m L_0 ,$$

$$2C_{2m} - \frac{W_s}{2W_B} \lambda_m L_0 (C_{1m} + C_{3m}) = 0 . \tag{2.20}$$

Hence,

$$C_{2m} = + \frac{W_s}{4W_B} \lambda_m L_0 \left(1 + G_m\right) C_{1m} ,$$

$$C_{3m} = G_m C_{1m} ,$$

$$C_{4m} = - \frac{W_s}{4W_B} \lambda_m L_0 \left(1 + G_m\right) C_{1m} , \qquad (2.21)$$

where

$$G_m = \frac{\sec \lambda_m L_0 \left(1 + \frac{W_s}{4W_B} \lambda_m L_0 \tanh \lambda_m L_0\right) + \frac{W_s}{4W_B} \lambda_m L_0 \operatorname{sech} \lambda_m L_0 \tan \lambda_m L_0}{\operatorname{sech} \lambda_m L_0 \left(1 - \frac{W_s}{4W_B} \lambda_m L_0 \tan \lambda_m L_0\right) - \frac{W_s}{4W_B} \lambda_m L_0 \sec \lambda_m L_0 \tanh \lambda_m L_0} . \qquad (2.22)$$

Substituting these equations into the general solution gives the equation defining $y_m^*(z)$ as

$$y_m^*(z) = C_{1m} \cosh \lambda_m z \left[1 + \frac{W_s}{4W_B} \lambda_m L_0 \left(1 + G_m\right) \tanh \lambda_m z + G_m \cos \lambda_m z \operatorname{sech} \lambda_m z - \frac{W_s}{4W_B} \lambda_m L_0 \left(1 + G_m\right) \sin \lambda_m z \operatorname{sech} \lambda_m z\right] \qquad (2.23)$$

for all odd values of m. The evaluation of the magnitude of C_{1m} will be discussed in Section 3.

m even; antisymmetric modes:

Let C_{1m}, C_{2m}, C_{3m}, C_{4m} be the constants of integration associated with the mth natural frequency ω_m. Directly substituting λ_m into the first three of Equations 2.10 and solving for the constants leads to:

$$- \left(C_{1m} + C_{3m}\right) + \lambda_m L_0 R^* \left(C_{2m} + C_{4m}\right) = 0 ,$$

$$\left[1 + \frac{W_s^*}{2W_B} R^* \left(\lambda_m L_0\right)^2\right] C_{1m} - \lambda_m L_0 R^* C_{2m} + \left[-1 + \frac{W_s^*}{2W_B} R^* \left(\lambda_m L_0\right)^2\right] C_{3m} + \lambda_m L_0 R^* C_{4m} = 0 ,$$

$$C_{1m} \cosh \lambda_m L_0 + C_{2m} \sinh \lambda_m L_0 - C_{3m} \cos \lambda_m L_0 - C_{4m} \sin \lambda_m L_0 = 0 . \qquad (2.24)$$

Hence,

$$C_{2m} = C_{1m}\left[\frac{2 + \frac{W_s^*}{2W_B} R^{*2} (\lambda_m L_0)^3 H_m}{R^* \lambda_m L_0 \left(2 - \frac{W_s^*}{2W_B} R^* (\lambda_m L_0)^2\right)}\right],$$

$$C_{3m} = C_{1m}\left[\frac{\frac{W_s^*}{2W_B} R^* (\lambda_m L_0)^2 + 2\lambda_m L_0 R^* H_m}{2 - \frac{W_s^*}{2W_B} R^* (\lambda_m L_0)^2}\right],$$

$$C_{4m} = C_{1m} H_m , \qquad (2.25)$$

where

$$R^* = \frac{R}{L_0}$$

$$W_s^* = \frac{I_s g}{R^2}$$

$$H_m = \frac{\left\{2 \sec \lambda_m L_0 \left(R^* \lambda_m L_0 + \tanh \lambda_m L_0\right) - \frac{W_s^*}{2W_B} R^{*2} (\lambda_m L_0)^3 \left(\sec \lambda_m L_0 + \operatorname{sech} \lambda_m L_0\right)\right\}}{\left\{R^* \lambda_m L_0 \left[2 \operatorname{sech} \lambda_m L_0 \left(R^* \lambda_m L_0 + \tan \lambda_m L_0\right) - \frac{W_s^*}{2W_B} R^* (\lambda_m L_0)^2 \left(\tanh \lambda_m L_0 \sec \lambda_m L_0 + \tan \lambda_m L_0 \operatorname{sech} \lambda_m L_0\right)\right]\right\}} \qquad (2.26)$$

Substituting these equations into the general solution gives the equation defining $y_m^*(z)$ as

$$y_m^*(z) = C_{1m} \cosh \lambda_m z \left\{1 + \left[\frac{2 + \frac{W_s^*}{2W_B} R^{*2} (\lambda_m L_0)^3 H_m}{R^* \lambda_m L_0 \left(2 - \frac{W_s^*}{2W_B} R^* (\lambda_m L_0)^2\right)}\right] \tanh \lambda_m z + \left[\frac{\frac{W_s^*}{2W_B} R^* (\lambda_m L_0)^2 + 2\lambda_m L_0 R^* H_m}{2 - \frac{W_s^*}{2W_B} R^* (\lambda_m L_0)^2}\right] \cos \lambda_m z \operatorname{sech} \lambda_m z + H_m \sin \lambda_m z \operatorname{sech} \lambda_m z\right\} \qquad (2.27)$$

for all even values of m.

3. CONSTRUCTION AND NORMALIZATION OF MODES

In the preceding section the functions $y_m^*(z)$, which are to be used to construct the symmetric and antisymmetric modes, have been derived up to the multiplicative constant C_{1m}. By following the rules outlined for the construction of $y_m(x)$, the mth natural mode of the system, and applying the orthonormalization condition, Equation 1.8, we can uniquely define the mth mode.

Figures 1 and 2 and the boundary conditions previously given show that the function $y_m^*(z)$, defined at every point in the interval

$$0 \leq z \leq L_0 ,$$

is identical with the function $y_m(x)$ at every point in the interval

$$L_0 + 2R \leq x \leq 2L ,$$

when

$$z = x - L_0 - 2R .$$

The determination of $y_m(x)$ over the full interval

$$0 \leq x \leq 2L$$

for the symmetric and the antisymmetric modes uses the following construction procedure:

m odd, symmetric modes:

For this case, the function $y_m^*(z)$ is defined by Equation 2.23 and

$$y_m(x) = \begin{cases} y_m^*(L_0 - x) , & \text{for} \quad 0 \leq x \leq L_0 \\ y_m^*(0) , & \text{for} \quad L_0 < x < L_0 + 2R \\ y_m^*(x - L_0 - 2R) , & \text{for} \quad L_0 + 2R \leq x \leq 2L . \end{cases} \tag{3.1}$$

m even, antisymmetric modes:

For this case, the function $y_m^*(z)$ is defined by Equation 2.27 and

$$y_m(x) = \begin{cases} -y_m^*(L_0 - x) , & \text{for} \quad 0 \leq x \leq L_0 \\ \frac{x - L}{R} y_m^*(0) , & \text{for} \quad L_0 < x < L_0 + 2R \\ y_m^*(x - L_0 - 2R) , & \text{for} \quad L_0 + 2R \leq x \leq 2L . \end{cases} \tag{3.2}$$

It will be recalled that $y_m(x)$ as constructed is defined only up to the multiplicative constant C_{1m}. This constant can be uniquely defined for each mode by requiring that the orthonormality condition

$$\int_0^{2L} \rho(x)\, y_m^2(x)\, dx = M_T \tag{3.3}$$

be satisfied for all m.

Besides predicting the deflection, we can predict the bending moment at each point of the system if we know the curvature of each mode. These are obtainable from the equation

$$y_m^{*\prime\prime}(z) = \lambda_m^2 \left(C_{1m} \cosh \lambda_m z + C_{2m} \sinh \lambda_m z - C_{3m} \cos \lambda_m z - C_{4m} \sin \lambda_m z\right) , \tag{3.4}$$

where the constants of integration are identical with those derived for $y_m(x)$. We can obtain the curvature of the mode $y_m(x)$ defined over the full system length by applying the construction rules that generated $y_m(x)$ from $y_m^*(z)$; that is, Equations 3.1 and 3.2.

4. TRANSIENT AND STEADY-STATE SOLUTIONS

With a complete set of modes, it is possible to derive a series solution for Equation 1.1—the equation of damped forced vibration of the entire system.

Substituting Equation 1.2 in Equation 1.1 gives

$$\sum_{n=1}^{\infty} \left[a_n(t) \frac{d^2}{dx^2} EI(x) \frac{d^2 y_n(x)}{dx^2} + \rho(x)\, y_n(x) \frac{d^2 a_n(t)}{dt^2} + \beta(x)\, y_n(x) \frac{da_n(t)}{dt} \right] = F(x, t) . \tag{4.1}$$

Using Equation 1.6 further reduces this to the form

$$\sum_{n=1}^{\infty} \left[\rho(x)\, y_n(x) \frac{d^2 a_n(t)}{dt^2} + 2\rho\zeta\omega_n\, y_n(x) \frac{da_n(t)}{dt} + \rho(x)\, y_n(x)\, \omega_n^2\, a_n(t) \right] = F(x, t) , \tag{4.2}$$

where the additional substitution

$$\beta(x) = 2\rho\zeta\omega_n \tag{4.3}$$

has also been made. The term ζ is commonly referred to as the "damping ratio" and is related to the constants of the system by Equation 4.3. It should be noted that the parameter ρ is the mass

per unit length of the beam alone. The equation states that $\beta(x)$ is independent of x; hence, energy is uniformly dissipated along the entire system length. This is an approximation, since actually zero energy is dissipated across the length of the rigid satellite body.

The summation and all dependence upon the coordinate x can be removed from Equation 4.2, by applying the orthonormality condition stated in Equation 1.8. Multiplying Equation 4.2 through by $y_n(x)$ and integrating over the entire system length reduces this equation to

$$\frac{d^2 a_n(t)}{dt^2} + 2\zeta_n \omega_n \frac{da_n(t)}{dt} + \omega_n^2 a_n(t) = \frac{\int_0^{2L} y_n(x) F(x, t)\, dx}{M_T}, \tag{4.4}$$

where ζ_n is the damping ratio associated with the nth mode and is given by

$$\zeta_n = \frac{\zeta}{M_T} \int_0^{2L} \rho y_n^2(x)\, dx . \tag{4.5}$$

n odd; symmetric modes excited:

$$\zeta_n = \frac{\zeta}{M_T} \int_0^{2L} \rho y_n^2(x)\, dx$$

$$= \zeta \left[1 - \frac{2W_T}{gM_T} y_n^2(0) - \frac{W_s}{gM_T} y_n^2(L_0)\right] . \tag{4.6}$$

n even; antisymmetric modes excited:

$$\zeta_n = \frac{\zeta}{M_T} \int_0^{2L} \rho y_n^2(x)\, dx$$

$$= \zeta \left[1 - \frac{2W_T}{gM_T} y_n^2(0) - \frac{W_s}{3gM_T} y_n^2(L_0)\right] . \tag{4.7}$$

Equation 4.4 is a differential equation that can be solved by means of the Laplace transform. Hence,

$$a_n(s) = \frac{\frac{1}{M_T} \int_0^{2L} y_n(x) F(x, s)\, dx}{s^2 + 2\zeta_n \omega_n s + \omega_n^2}, \tag{4.8}$$

where

$$\mathcal{L}\{F(x, t)\} = F(x, s)$$

$$\mathcal{L}\{a_n(t)\} = a_n(s) \tag{4.9}$$

and the initial values of $a_n(t)$ are assumed equal to zero.

The system being linear means that we can use the principle of superposition to determine the actual system response to the force distribution $F(x, t)$, by adding the response due to each individual force distribution of an equivalent force system.

Let the equivalent force system be defined by the two force distributions $F_1(x, t)$ and $F_2(x, t)$, where

$F_1(x, t) = F_1(x) f(t)$ = a force distribution of periodic intensity that is symmetric about the system's axis of symmetry and excites only the symmetric modes of vibration,

$F_2(x, t) = F_2(x) f(t)$ = a force distribution of periodic intensity that is antisymmetric about the system's axis of symmetry and excites only the antisymmetric modes of vibration.

The function $f(t)$ appearing above is a continuous function of time; it describes the intensity of the force distribution $F_1(x, t)$ and $F_2(x, t)$ at time t. It will be assumed for this analysis that $f(t)$ is periodic with period t_2 and expressible as a Fourier series. That is,

$$f(t) = \frac{1}{2} b_0 + \sum_{m=1}^{\infty} \left(b_m \cos \frac{2m\pi}{t_2} t + d_m \sin \frac{2m\pi}{t_2} t \right), \tag{4.10}$$

where b_m and d_m are the Fourier coefficients associated with the function $f(t)$ given by:

$$b_m = \frac{2}{t_2} \int_0^{t_2} f(t) \cos \frac{2m\pi}{t_2} t \, dt \qquad m = 0, 1, 2 \cdots \tag{4.11}$$

$$d_m = \frac{2}{t_2} \int_0^{t_2} f(t) \sin \frac{2m\pi}{t_2} t \, dt \qquad m = 1, 2, \cdots \tag{4.12}$$

$F(x, t)$ as it appears in Equation 4.8 can be replaced by the equivalent-force system defined above. Then, a direct substitution of Equation 4.10 in Equation 4.8 yields an expression that can

be readily inverted by convolution:

$$a_n(t) = \frac{K_n}{M_T \omega_n \left(1-\zeta_n^2\right)^{1/2}} \left[\frac{1}{2} b_0 + \sum_{m=1}^{\infty} \left(b_m \cos \frac{2m\pi}{t_2} t + d_m \sin \frac{2m\pi}{t_2} t\right)\right] * e^{-\zeta_n \omega_n t} \sin \omega_n \left(1-\zeta_n^2\right)^{1/2} t \quad , \quad (4.13)$$

where

n odd; symmetric modes:

$$K_n = \int_0^{2L} y_n(x) F_1(x)\, dx \quad (4.14)$$

n even; antisymmetric modes:

$$K_n = \int_0^{2L} y_n(x) F_2(x)\, dx \quad (4.14a)$$

and "*" is the symbol used to denote convolution.

Once evaluated, the expression for $a_n(t)$ can be substituted in Equation 1.2 and the displacement at any point x along the system calculated for any time t. Furthermore, differentiating Equation 1.2 twice and multiplying the results by EI gives the bending moment at any point for any time t.

Letting

$\Omega_n = \omega_n \left(1-\zeta_n^2\right)^{1/2}$ = damped natural frequency of nth mode,

$\nu_n = \zeta_n \omega_n$ = inverse of time constant for nth mode,

$\theta = 2\pi/t_2$ = frequency of applied-force distribution,

and performing the convolution operation called for in Equation 4.13, leads to

$$a_n(t) = \frac{K_n}{M_T \Omega_n}\left\{\frac{1}{2} b_0 \int_0^t e^{-\nu_n \tau} \sin \Omega_n \tau \, d\tau + \sum_{m=1}^{\infty}\left[b_m \int_0^t \cos m\theta(t-\tau)\, e^{-\nu_n \tau} \sin \Omega_n \tau \, d\tau + d_m \int_0^t \sin m\theta(t-\tau)\, e^{-\nu_n \tau} \sin \Omega_n d\tau\right]\right\} \quad (4.16)$$

$$= \frac{K_n}{2M_T \Omega_n}\left\{b_0\left[\frac{\Omega_n}{\nu_n^2 + \Omega_n^2} - \frac{e^{-\nu_n t}\left(\nu_n \sin \Omega_n t + \Omega_n \cos \Omega_n t\right)}{\nu_n^2 + \Omega_n^2}\right]\right.$$

$$+ \sum_{m=1}^{\infty} b_m \left[\frac{\left(\Omega_n - m\theta\right) \cos m\theta t + \nu_n \sin m\theta t}{\nu_n^2 + \left(\Omega_n - m\theta\right)^2} - \frac{e^{-\nu_n t}\left[\nu_n \sin \Omega_n t + \left(\Omega_n - m\theta\right) \cos \Omega_n t\right]}{\nu_n^2 + \left(\Omega_n - m\theta\right)^2}\right.$$

$$\left. + \frac{\left(\Omega_n + m\theta\right) \cos m\theta t - \nu_n \sin m\theta t}{\nu_n^2 + \left(\Omega_n + m\theta\right)^2} - \frac{e^{-\nu_n t}\left[\nu_n \sin \Omega_n t + \left(\Omega_n + m\theta\right) \cos \Omega_n t\right]}{\nu_n^2 + \left(\Omega_n + m\theta\right)^2}\right]$$

$$+ \sum_{m=1}^{\infty} d_m \left[\frac{\left(\Omega_n - m\theta\right) \sin m\theta t - \nu_n \cos m\theta t}{\nu_n^2 + \left(\Omega_n - m\theta\right)^2} + \frac{e^{-\nu_n t}\left[\nu_n \cos \Omega_n t - \left(\Omega_n - m\theta\right) \sin \Omega_n t\right]}{\nu_n^2 + \left(\Omega_n - m\theta\right)^2}\right.$$

$$\left.\left. + \frac{\left(\Omega_n + m\theta\right) \sin m\theta t + \nu_n \cos m\theta t}{\nu_n^2 + \left(\Omega_n + m\theta\right)^2} - \frac{e^{-\nu_n t}\left[\nu_n \cos \Omega_n t - \left(\Omega_n + m\theta\right) \sin \Omega_n t\right]}{\nu_n^2 + \left(\Omega_n + m\theta\right)^2}\right]\right\} . \quad (4.17)$$

This equation for $a_n(t)$ can be used to define the transient response of the system when initially at rest and then set in vibration by the defined applied force $F(x, t)$. In order to investigate the response at the point x of the system at time t, we substitute Equation 4.17 in

$$Y(x, t) = \sum_{n=1}^{\infty} a_n(t)\, y_n(x) , \quad (4.18)$$

to yield the transverse displacement, and in

$$EI\, Y''(x, t) = EI \sum_{n=1}^{\infty} a_n(t)\, y_n''(x) \quad (4.19)$$

to yield the bending moment.

By observing how each term

$$a_n(t)\,y_n(x) \tag{4.20}$$

and

$$EI\,a_n(t)\,y_n''(x) \tag{4.21}$$

changes as a function of time, the contribution to the total response from each individual mode can be ascertained for the particular forcing function in question.

In addition to the transient response, the steady-state response of each mode to the particular forcing function is of interest. In deriving the resultant steady-state response of the system, note that the steady-state generalized coordinate $a_n(t)_{ST}$ given by

$$a_n(t)_{ST} = \frac{K_n}{2M_T\Omega_n}\left\{\frac{b_0\,\Omega_n}{\nu_n^2+\Omega_n^2} + \sum_{m=1}^{\infty} b_m\left[\frac{(\Omega_n - m\theta)\cos m\theta t + \nu_n \sin m\theta t}{\nu_n^2+(\Omega_n+m\theta)^2} + \frac{(\Omega_n+m\theta)\cos m\theta t - \nu_n \sin m\theta t}{\nu_n^2+(\Omega_n+m\theta)^2}\right]\right.$$

$$\left. + \sum_{m=1}^{\infty} d_m\left[\frac{(\Omega_n - m\theta)\sin m\theta t - \nu_n \cos m\theta t}{\nu_n^2+(\Omega_n-m\theta)^2} + \frac{(\Omega_n+m\theta)\sin m\theta t + \nu_n \cos m\theta t}{\nu_n^2+(\Omega_n+m\theta)^2}\right]\right\} \tag{4.22}$$

is not necessarily in phase at the steady-state time t for all n, since it is obtained by evaluating $a_n(t)$ with the exponential terms deleted.

5. SOLUTION TO FREQUENCY EQUATION

It has been shown that the frequency equation associated with the symmetric modes of vibration of the entire system is

$$\frac{W_T}{W_B} = -\frac{\tanh\lambda L_0 + \tan\lambda L_0 + \frac{W_s}{2W_B}\lambda L_0\left(1+\sec\lambda L_0\,\mathrm{sech}\,\lambda L_0\right)}{2\lambda L_0 - \frac{W_s}{2W_B}(\lambda L_0)^2\left(\tan\lambda L_0 - \tanh\lambda L_0\right)}, \tag{5.1}$$

and the frequency equation associated with the antisymmetric modes of vibration of the entire system is

$$\frac{W_T}{W_B} = \frac{\left\{\tanh \lambda L_0 - \tan \lambda L_0 - 2\lambda L_0 R^* \tan \lambda L_0 \tanh \lambda L_0 - (\lambda L_0 R^*)^2 (\tanh \lambda L_0 + \tan \lambda L_0) - \frac{I_s}{3I_B} (\lambda L_0)^3 (1 + \sec \lambda L_0 \operatorname{sech} \lambda L_0)\right\}}{\left\{\lambda L_0 \left[2 \tan \lambda L_0 \tanh \lambda L_0 + 2R^* \lambda L_0 (\tanh \lambda L_0 + \tan \lambda L_0) + 2(R^* \lambda L_0)^2 + \frac{I_s}{3I_B} (\lambda L_0)^3 (\tanh \lambda L_0 - \tan \lambda L_0)\right]\right\}} . \quad (5.2)$$

By the proper definition of the parameters contained in these equations it is possible to predict the natural frequencies of any system that may be modeled as the symmetric double-beam system shown in Figure 1. If the system to be modeled as a double-beam system has four or more elastic members attached to a rigid central body, the frequency equations given above yield only those frequencies associated with the system mode shapes that are similar to the symmetric and antisymmetric modes defined.

The physical parameters needed to solve the frequency equations of the double beam model are:

W_s = weight of rigid satellite body (without beams and tip weights),

I_s = mass moment of inertia of rigid satellite body (without beams and tip weights) about the axis through the center of mass and normal to the plane of vibration,

I_B = mass moment of inertia of a beam, of length $2L_0$, about an axis normal to the length and passing through its centroid,

W_T = tip weight,

L_0 = length of a single beam,

ρ = mass per unit length of beam,

EI = bending stiffness of beam,

R = radius of symmetric satellite body,

g = acceleration of gravity.

Equations 5.1 and 5.2 show that the solutions to the frequency equations will depend only on the magnitudes of four distinct dimensionless ratios.

In particular, the solutions for the symmetric modes involves parameters

$$\frac{W_T}{W_B}, \qquad \frac{W_s}{W_B},$$

while the solutions for the antisymmetric modes involves

$$\frac{W_T}{W_B}, \qquad \frac{I_s}{I_B}, \quad R^* .$$

These can be calculated for the symmetric double-beam system from the above definitions and the equations

$$W_B = \rho g L_0 \ ,$$

$$R^* = \frac{R}{L_0} \ ,$$

$$I_B = \frac{2}{3} \rho L_0^3 \ ., \tag{5.3}$$

Figures 3 through 7 attempt to provide sufficient information so that Equations 5.1 and 5.2 may be accurately solved for all practical values of the defined ratios. With these approximate solutions and the relation

$$\omega = \frac{(\lambda L_0)^2}{L_0^2} \sqrt{\frac{EI}{\rho}} \tag{5.4}$$

it is possible to obtain a very good estimate of the first few natural frequencies of the satellite system in question.

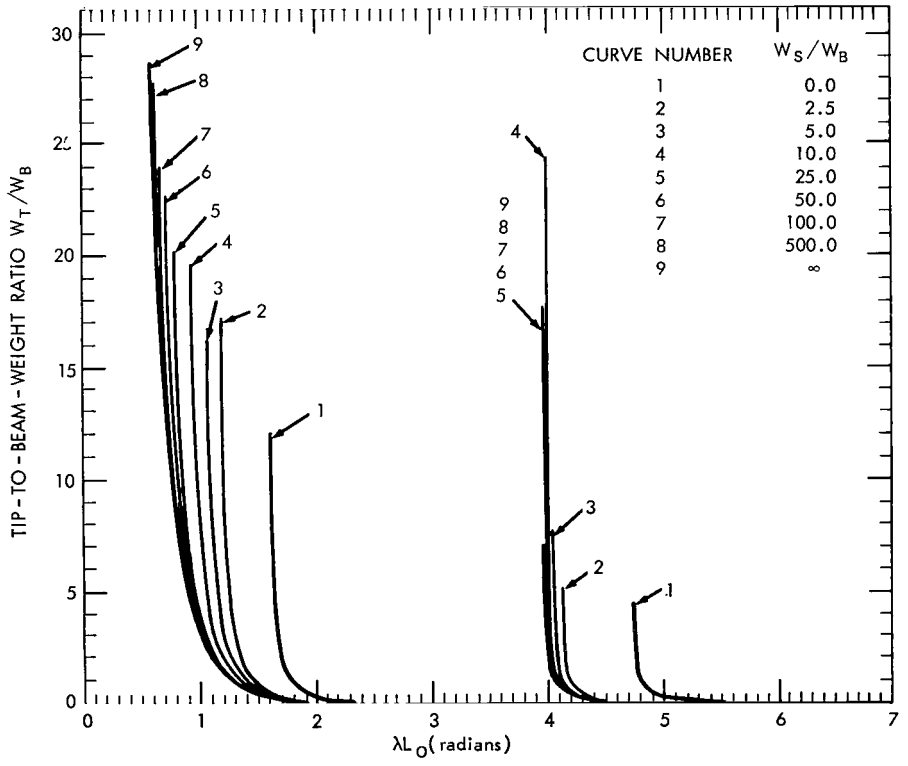

Figure 3—Symmetric mode, W_T/W_B vs λL_0 for different values of W_s/W_B.

Each curve labeled in Figure 3 plots W_T/W_B vs λL_0 as obtained from Equation 5.1 for the values of W_s/W_B tabulated on the figure. This figure contains sufficient information to give an accurate estimate of the first two values of λL_0 that satisfy Equation 5.1. The natural frequencies associated with the estimated values of λL_0 correspond to the first two modes of vibration for which the satellite body can translate but not rotate. For the double-boom system, these are the first two symmetric modes of vibration.

A set of curves which provide sufficient information to accurately estimate the natural frequencies associated with the antisymmetric modes of vibration can be obtained by plotting W_T/W_B vs λL_0 (as derived via Equation 5.2) for incremental values of both I_s/I_B and R^* in the range

$$0 \leq \frac{I_s}{I_B} < \infty$$

and

$$0 < R^* \leq 0.10 .$$

Since this involves incrementally varying three parameters; the following approach is used to present the results in a more compact form.

Intuitively one fells that the least critical parameter appearing in Equation 5.2 is R^*. That is, for satellites having long elastic members such that

$$0 < R^* \leq 0.1 ,$$

the natural frequencies will be essentially the same, no matter what the exact value of R^* may be.

Figures 4 and 5 lend graphic support to this intuitive notion and thus provide one with sufficient information to determine the magnitude range of inertia ratio I_s/I_B over which R^* plays an insignificant role in the estimation of the system's first two antisymmetric modal frequencies. That is, we show how sensitive the asymptotes and zero crossings of Equation 5.2 are to change in I_s/I_B and R^*. Since it will be shown that the curves W_T/W_B vs λL_0 as derived from Equation 5.2 have shapes similar to those shown in Figure 3, it may be inferred that any intermediate value of W_T/W_B between zero and infinity will exhibit the same sensitivity to changes in I_s/I_B and R^* as do the asymptotes and zero crossings.

Figure 4 plots I_s/I_B vs λL_0 for the values of R^* tabulated on the figure. These curves are obtained from Equation 5.2 when W_T/W_B is set equal to infinity; that is, from

$$\frac{I_s}{I_B} = \frac{6\left[\tan\lambda L_0 \tanh\lambda L_0 + R^*\lambda L_0\left(\tanh\lambda L_0 + \tan\lambda L_0\right) + \left(R^*\lambda L_0\right)^2\right]}{\left(\lambda L_0\right)^3\left(\tan\lambda L_0 - \tanh\lambda L_0\right)} . \qquad (5.5)$$

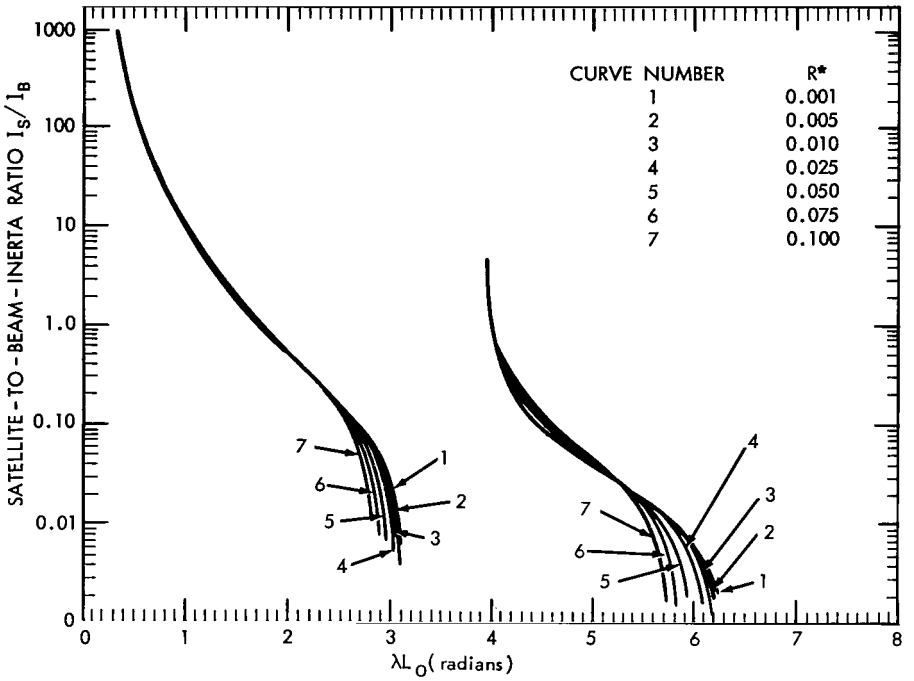

Figure 4—Antisymmetric mode, I_s/I_B vs λL_0 for different values of R*, when $W_T/W_B = \infty$.

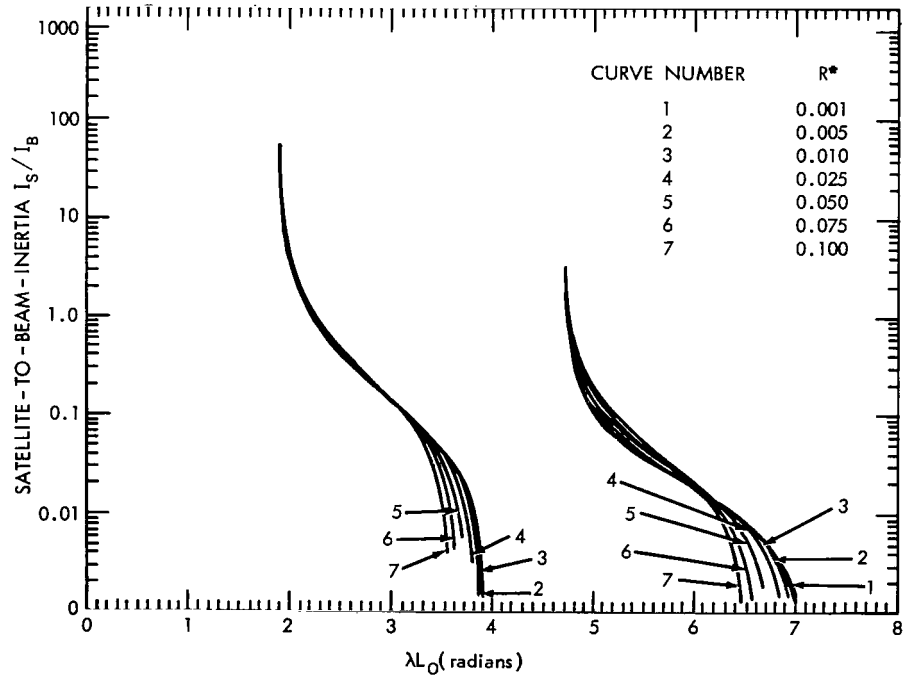

Figure 5—Antisymmetric mode, I_s/I_B vs λL_0 for different values of R*, when $W_T/W_B = 0$.

Similarly Figure 5 plots I_s/I_B vs λL_0 for the same values of R^*, as obtained from Equation 5.2 when W_T/W_B is set equal to zero; that is, from

$$\frac{I_s}{I_B} = \frac{3\left[\tanh\lambda L_0 - \tan\lambda L_0 - 2R^*\lambda L_0 \tan\lambda L_0 \tanh\lambda L_0 - (R^*\lambda L_0)^2\,(\tanh\lambda L_0 + \tan\lambda L_0)\right]}{(\lambda L_0)^3\,(1 + \sec\lambda L_0 \operatorname{sech}\lambda L_0)} \quad . \tag{5.6}$$

Making use of the fact that the solutions to Equation 5.2 are virtually insensitive to changes in the parameter R^* over the limits defined, Figures 6 and 7 plot W_T/W_B vs λL_0 as derived from Equation 5.2 for the values of $R^* = 0.01$ and $R^* = 0.10$ respectively and the values of I_s/I_B listed on the figure. These figures contain sufficient information to give accurate estimates of the first two values of λL_0 that satisfy Equation 5.2 for any system that can be modeled as discussed. The natural frequencies associated with the estimated values of λL_0 correspond to the first two modes of vibration for which the satellite body can rotate but not translate. For the double-beam system these are the first two antisymmetric modes of vibration.

Aside from providing the information needed for solving both frequency equations, Figures 3 through 7 along with Equation 5.4 provide quantitative and qualitative insight as to how changes in the system parameters will change the system's natural frequencies.

The range of W_s/W_B values listed on Figure 3 shows that the root boundary conditions for the symmetric modes vary between zero satellite weight (guided root) and infinite satellite weight (clamped root). Similarly, the range of the ratio magnitudes listed on Figures 6 and 7 show that the root boundary conditions for the antisymmetric modes vary between zero satellite rotational inertia (hinged root) to infinite rotational inertia (clamped root) for each of the listed ratios R^*. For both cases, the variation in the tip boundary conditions from zero tip weight (free tip) to infinite tip weight (hinged tip) is illustrated by choosing W_T/W_B as the vertical axis of Figures 3, 6, and 7.

Figure 8 gives a ready reference for the general solution of the frequency equations in the limiting cases mentioned above. The figure shows the schematic diagram of each limiting case along with the solutions to its frequency equation. Reference 3 gives the solutions for these cases, also for cases corresponding to other common beam boundary conditions.

Figures 3 through 7 and Equation 5.4 suggest the following observations:

1. The solutions λL_0 of the frequency equations are independent of the bending stiffness EI. Thus the system's natural frequencies are directly proportional to the square root of the bending stiffness.

2. The solutions λL_0 of the frequency equations have nonlinear dependence on the boom weight W_B. Thus a simple proportionality relation between boom length L_0 or mass distribution ρ and the natural frequencies exists only in special cases.

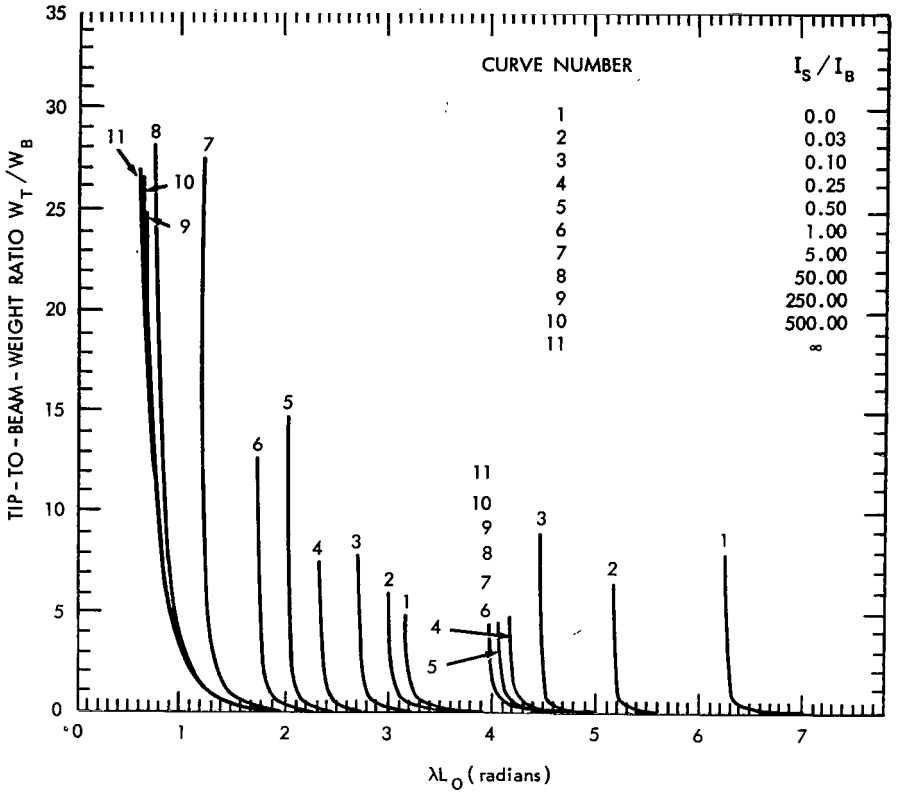

Figure 6—Antisymmetric mode, W_T/W_B vs λL_0 for different values of I_s/I_B, when $R^* = 0.01$.

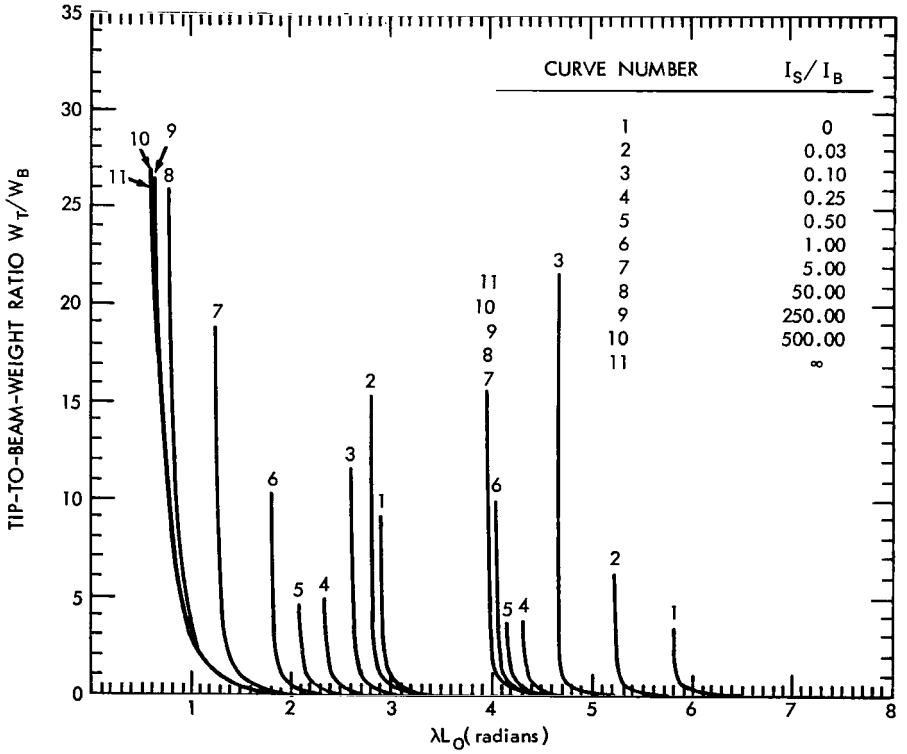

Figure 7—Antisymmetric mode, W_T/W_B vs λL_0 for different values of I_s/I_B, when $R^* = 0.10$.

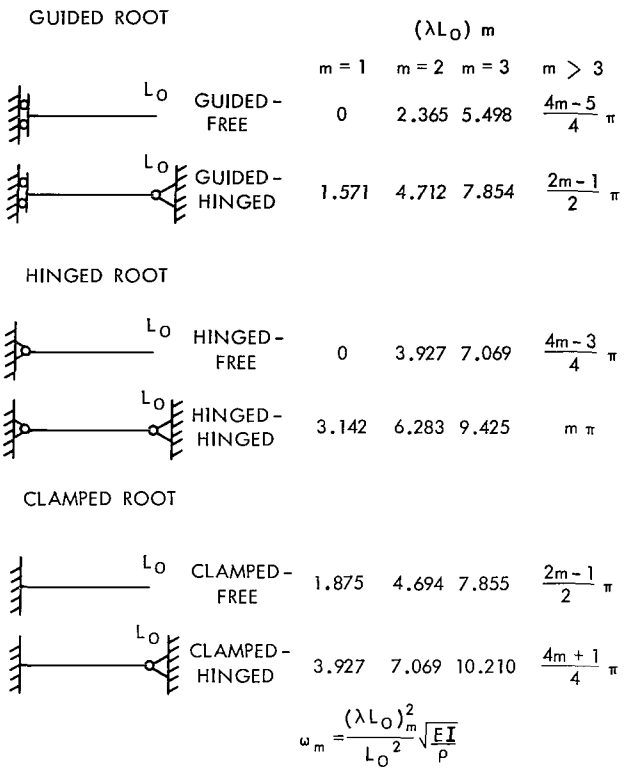

Figure 8—Natural frequencies of uniform beams with different boundary conditions.

3. As the satellite-to-beam-weight ratio W_s/W_B increases, the solution $(\lambda L_0)_1$ associated with the first symmetric mode of vibration approaches the value that results from a clamped-root condition. Figure 3 shows that for W_s/W_B greater than 100 and W_T/W_B less than 20 the root may be assumed clamped and the frequency associated with the first symmetric mode of vibration is approximately that of a clamped beam with tip weight.

4. Figures 4 and 5 show that for satellites having a satellite-to-beam-length ratio R* in the interval

$$0 < R^* \leq 0.10 ,$$

the solution $(\lambda L_0)_2$ associated with the first antisymmetric mode of vibration will be essentially independent of the magnitude of R* for all inertia ratios I_s/I_B greater than 0.10. For the range

$$\frac{I_s}{I_B} < 0.10$$

and

$$0.05 < R^* < 0.10 ,$$

the quantity R* becomes a significant parameter in Equation 5.2. This situation implies that the satellite's rotational inertia is small compared with the boom's; at the same time, the boom cannot be extremely long compared with the length of the rigid satellite body (a situation approaching that of a physically unrealistic system). Thus, for most actual satellites, the magnitude of R* and hence the actual satellite body size will be of second order importance in predictions of the system's first antisymmetric modal frequency.

5. Figures 6 and 7 show that as the satellite inertia-to-beam inertia ratio I_s/I_B increases, the solution $(\lambda L_0)_2$ associated with the first antisymmetric mode of vibration approaches the value

that results from the clamped-root condition defined by curve number 11 on both figures. The inertia ratio needed to effectively clamp the root and hence restrict the rotational motion of the satellite body is extremely large and strongly dependent on the tip-to-beam-weight ratio W_T/W_B. For example, if $W_T/W_B = 1$, then the inertia ratio I_s/I_B must be greater than 50 for the root to be considered clamped.

6. Comparing the values of $(\lambda L_0)_2$ that define the asymptotes of the curves shown in Figures 6 and 7 with the true values of the asymptotes given in Figure 4 shows that for every satellite having an inertia ratio I_s/I_B less than 5, a tip-to-beam-weight ratio can be found such that the system will vibrate as if the system had infinitely heavy tip weights. For example, if the inertia ratio of the satellite were less than 1, then the system would vibrate as if its tips were pinned in inertial space by infinitely heavy tip weights, for any W_T/W_B greater than 5.

7. As W_T/W_B increases from 0 to 3, the solutions $(\lambda L_0)_n$, $n = 3, 4, \cdots$ of the frequency equations, associated with the second and higher symmetric and antisymmetric modes, undergo a rapid decrease irrespective of satellite body weight, size, and rotational inertia. As W_T/W_B is increased beyond 3, $(\lambda L_0)_n$ becomes insensitive to any further change and approaches the solution associated with the case of a hinged tip. Thus, if the tip-to-beam-weight ratio exceeds 3, the symmetric double-beam system will have its tips effectively hinged in inertial space for the third and all higher modes of vibration.

6. DYNAMIC RESPONSE OF ATS-D

The introduction stated that this paper would solve a particular problem: to determine whether the microthruster on ATS-D could excite a resonant response of sufficient magnitude to buckle the long elastic members (booms) attached to the spacecraft body.

In order to introduce conservatism into the model and reduce the problem to a form compatible with this analysis, we make some simplifying assumptions:

1. The actual satellite deploying four booms with tip weights may be adequately approximated by the symmetric double-beam system.

2. The microthruster acts normal to the system at the point on the satellite body coincident with the point at which one of the beams is clamped. The intensity of the microthruster may be approximated by a periodic triangular wave having a rise time unequal to the decay time and a peak intensity of one micropound.

Let

t_1 = rise time of triangular wave, sec,

t_2 = period of triangular wave, sec,

10^{-6} = one micropound, lb,

$\delta(x)$ = Dirac Delta function.

Then the actual applied force distribution $F(x, t)$ is described by

$$F(x, t) = \delta(x - L - R)\, f(t) , \tag{6.1}$$

where, in the time interval

$$0 \leq t \leq t_2 ,$$

$$f(t) = 10^{-6} \frac{t}{t_1} \qquad \text{for} \quad 0 \leq t \leq t_1$$

$$f(t) = 10^{-6} \left(\frac{t_2 - t}{t_2 - t_1}\right) \quad \text{for} \quad t_1 < t \leq t_2 . \tag{6.2}$$

This force distribution is replaced in the analysis by the equivalent force system described by $F_1(x, t)$ and $F_2(x, t)$; that is:

$$F_1(x,t) = F_1(x)f(t) = \delta(L - x)f(t) \tag{6.3}$$

$$F_2(x,t) = F_2(x)f(t) = \left[\delta\left(L + \frac{R}{2} - x\right) - \delta\left(L - \frac{R}{2} - x\right)\right] f(t). \tag{6.4}$$

where

$F_1(x, t)$ = force applied at the center of mass,

$F_2(x, t)$ = couple applied about the center of mass.

It follows from Equations 4.11, 4.12, and 6.2 that the Fourier coefficients described in Section 4 are:

$$b_0 = 10^{-6}$$

$$b_m = -\left[\frac{10^{-6} t_2^2}{2m^2 \pi^2 t_1 (t_2 - t_1)}\right] \left(1 - \cos \frac{2m\pi}{t_2} t_1\right) ,$$

$$d_m = \left[\frac{10^{-6} t_2^2}{2m^2 \pi^2 t_1 (t_2 - t_1)}\right] \sin \frac{2m\pi}{t_2} t_1 , \qquad m = 1, 2, \ldots \tag{6.5}$$

and that the constants K_n described by Equations 4.14, 4.14a, 6.3, and 6.4 are:

n odd; symmetric modes:

$$K_n = y_n(L) , \tag{6.6}$$

n even; antisymmetric modes:

$$K_n = y_n\left(L + \frac{R}{2}\right) - y_n\left(L - \frac{R}{2}\right) . \tag{6.7}$$

3. The vibrational motion will be damped by the internal friction of the boom material only and this is describable by a viscous-type damping term in the analysis. Reference 4 presents the results of experiments aimed at precisily defining the magnitude of the damping coefficient ζ for De Havilland-type booms. It may be concluded from this that worst-case-type results may be obtained by setting

$$\zeta = 10^{-4} . \tag{6.8}$$

4. The adjusted geometric and physical parameters that describe the double-beam model of the four boom ATS-D satellite are assumed to be approximated by the magnitudes listed in Table 1. It must be noted that the mass distribution, bending stiffness, and tip weight of the beam are exactly twice the corresponding values for a single boom of the actual satellite system.

Table 1

Adjusted Parameters for Double-Beam Model of ATS-D.

Symbol	Parameter	Value
ρ	Mass distribution of boom	0.8125×10^{-3} slugs ft^{-1}
EI	Bending stiffness of boom	26 lbs ft^2
L_0	Boom length	123.5 ft
R	Radius of ATS	2 ft
W_T	Tip weight	16 lb
W_s	Weight of ATS (without booms and tip weights)	641.4 lb
I_s	Rotational inertia of ATS (without booms and tip weights)	76.9 slugs ft^2

To give accurate values of the first n natural frequencies of the double-beam system, Equations 5.1 and 5.2 must be solved numerically. It will be recalled that Equation 5.1 is the frequency equation for the symmetric modes and that Equation 5.2 is the frequency equation for the antisymmetric modes.

Table 2 lists the first ten values of λL_0 that satisfy these equations. The odd-numbered values correspond to the solutions to Equation 5.1, and the even-numbered values correspond to the solutions

Table 2

First Ten Natural Frequencies of ATS-D.

$(\lambda L_0)_n$ (radian)		ω_n (radian sec^{-1})		T_n (sec)	
$(\lambda L_0)_1$	0.88243	ω_1	0.009133	T_1	687.99
$(\lambda L_0)_2$	2.8137	ω_2	0.09285	T_2	67.670
$(\lambda L_0)_3$	3.9815	ω_3	0.18592	T_3	33.794
$(\lambda L_0)_4$	4.6516	ω_4	0.25378	T_4	24.759
$(\lambda L_0)_5$	7.1223	ω_5	0.59495	T_5	10.561
$(\lambda L_0)_6$	7.2675	ω_6	0.61945	T_6	10.143
$(\lambda L_0)_7$	10.2635	ω_7	1.2355	T_7	5.0857
$(\lambda L_0)_8$	10.3144	ω_8	1.2477	T_8	5.0356
$(\lambda L_0)_9$	13.4048	ω_9	2.1075	T_9	2.9814
$(\lambda L_0)_{10}$	13.4291	ω_{10}	2.1151	T_{10}	2.9706

to Equation 5.2. The table also lists the modal frequency and period associated with each solution $(\lambda L_0)_n$.

Both the symmetric and antisymmetric mode shapes of the entire system can be generated by using the values of $(\lambda L_0)_n$ listed in Table 2 and the other quantities given in Table 1.

Figures 9 through 13 plot the normalized displacement $y_n(x)$ vs the position coordinate x for the first five symmetric modes. The equations used to define these mode shapes are obtained by evaluating Equation 2.23 for those λL_0's with odd subscripts listed in Table 2, applying the construction rules given by Equations 3.1, and normalizing according to Equation 3.3.

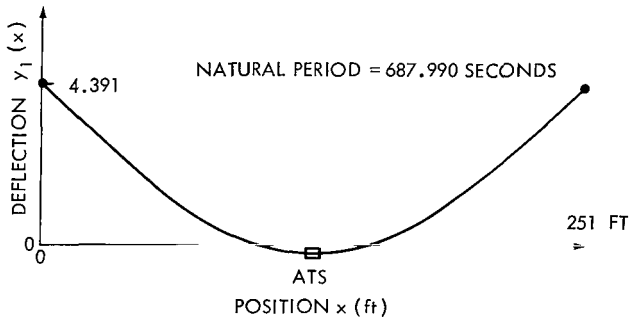

Figure 9—First symmetric mode of ATS system described in Table 1.

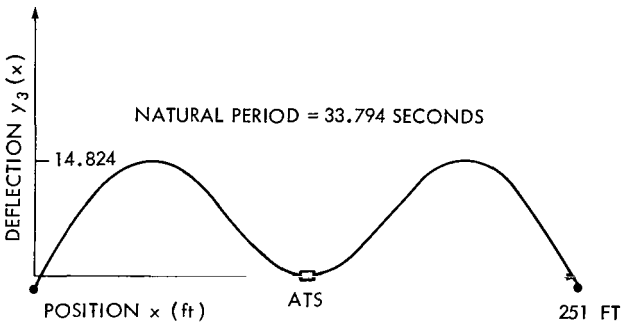

Figure 10—Second symmetric mode of ATS system described in Table 1.

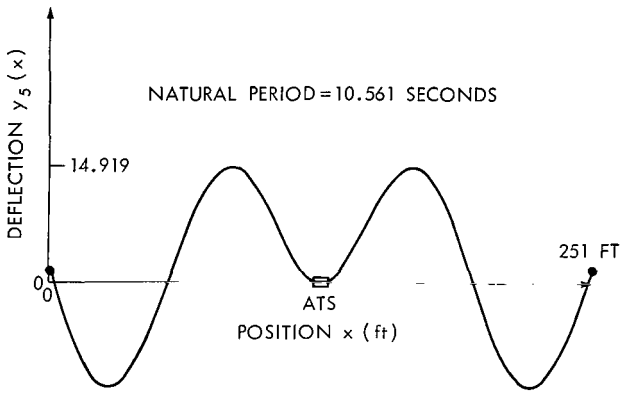

Figure 11—Third symmetric mode of ATS system described in Table 1.

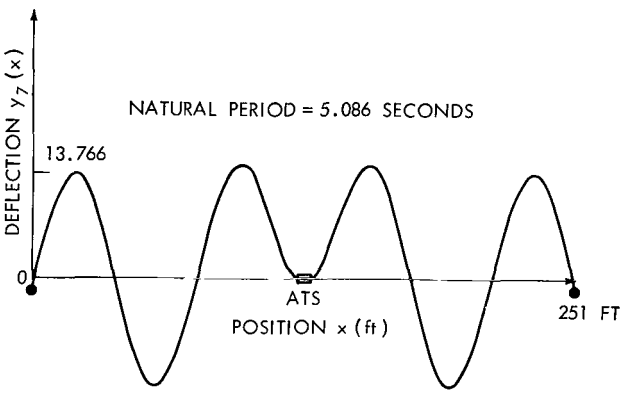

Figure 12—Fourth symmetric mode of ATS system described in Table 1.

Figures 14 through 18 plot the normalized displacement $y_n(x)$ vs position coordinate x for the first five antisymmetric modes. The equations used to define these mode shapes are obtained by evaluating Equation 2.27 for those λL_0's with even subscripts listed in Table 2, applying the construction rules given by Equation 3.2, and normalizing according to Equation 3.3.

Besides the mode shapes of the system, it is also possible to generate equations that define the normalized curvature of every point along each mode shape. This may be done by

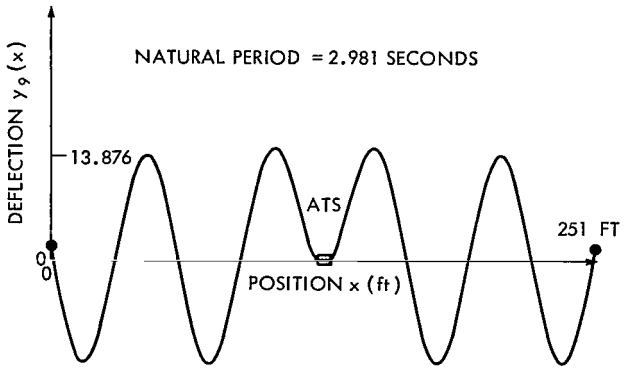

Figure 13—Fifth symmetric mode of ATS system described in Table 1.

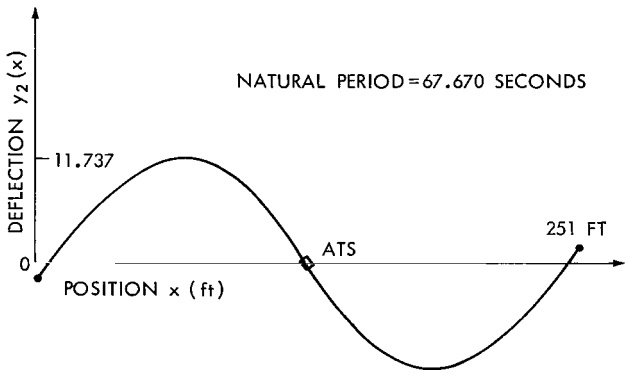

Figure 14—First antisymmetric mode of ATS system described in Table 1.

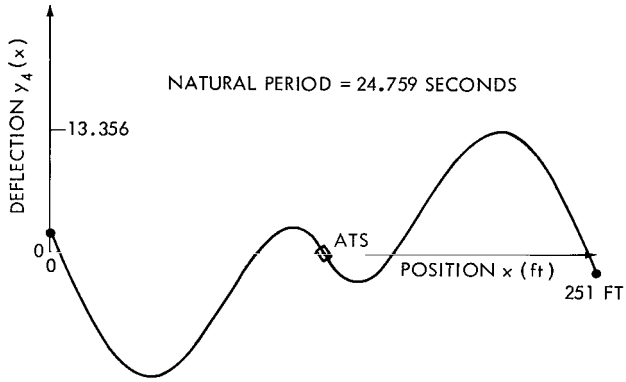

Figure 15—Second antisymmetric mode of ATS system described in Table 1.

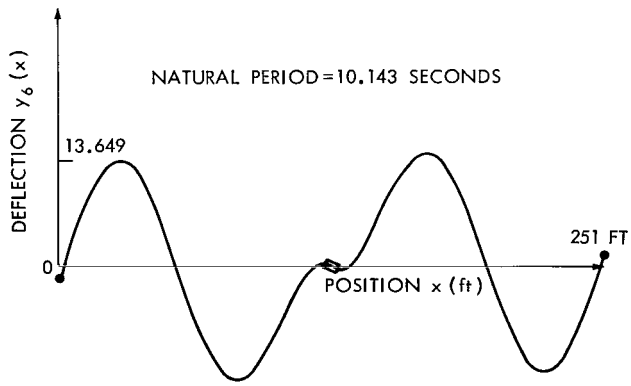

Figure 16—Third antisymmetric mode of ATS system described in Table 1.

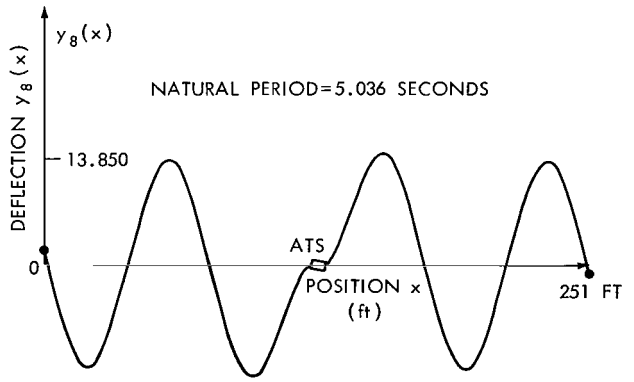

Figure 17—Fourth antisymmetric mode of ATS system described in Table 1.

substituting the values of C_{1n} determined from the normalization of $y_n(x)$ in Equation 2.21 or 2.25 to determine C_{2n}, C_{3n}, and C_{4n}. These normalized constants can then be substituted in Equation 3.4 to give an expression for $y_n''(z)$. This resulting expression can be substituted in Equation 3.1 or 3.2, depending on whether n is odd or even, respectively, to construct $y_n''(x)$, the normalized curvature of the nth mode.

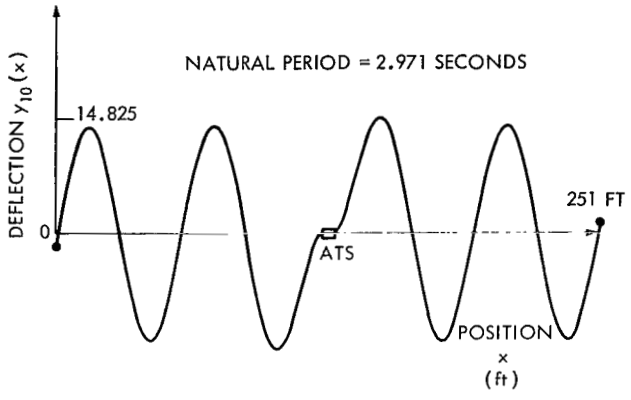

Figure 18—Fifth antisymmetric mode of ATS system described in Table 1.

Figures 19 through 23 plot the normalized curvature $y_n''(x)$ of the first five symmetric modes of the system (n odd) vs position coordinate x.

Figures 24 through 28 plot the normalized curvature $y_n''(x)$ of the first five antisymmetric modes of the system (n even) vs position coordinate x.

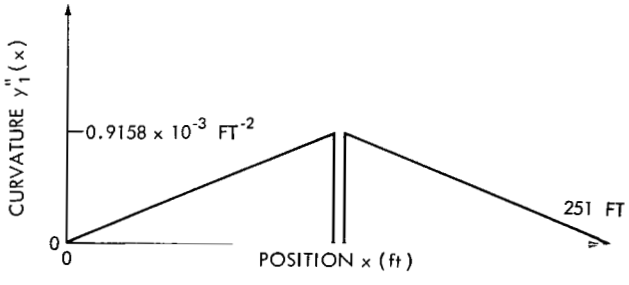

Figure 19—Curvature of first symmetric mode.

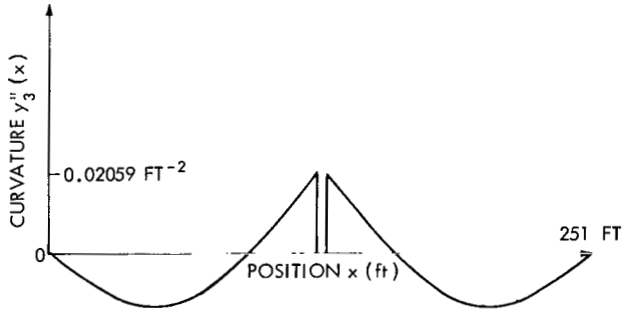

Figure 20—Curvature of second symmetric mode.

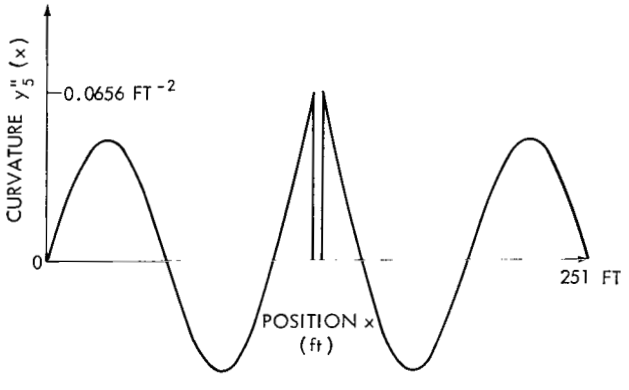

Figure 21—Curvature of third symmetric mode.

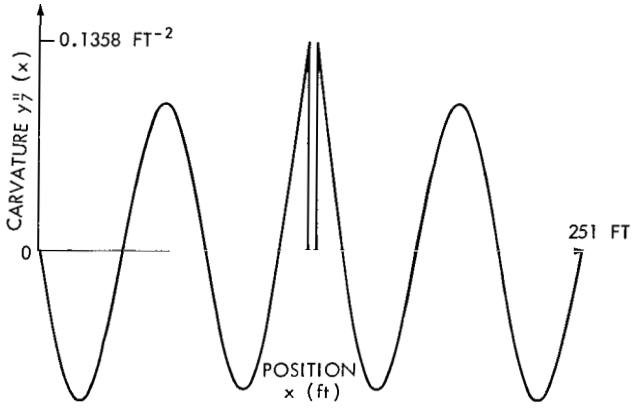

Figure 22—Curvature of fourth symmetric mode.

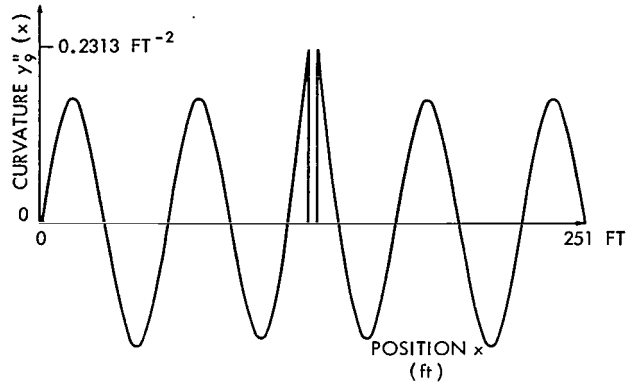

Figure 23—Curvature of fifth symmetric mode.

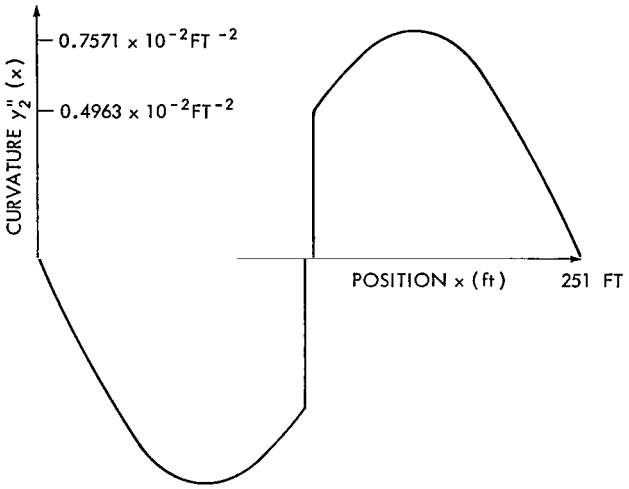

Figure 24—Curvature of first antisymmetric mode.

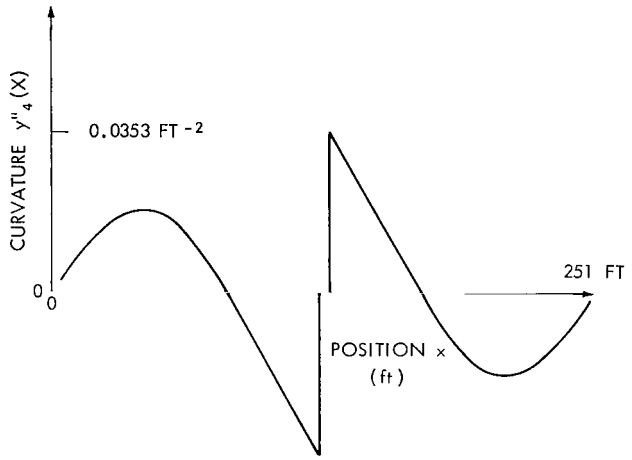

Figure 25—Curvature of second antisymmetric mode.

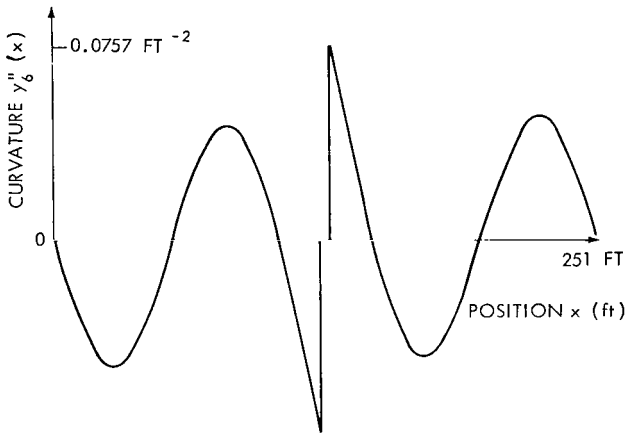

Figure 26—Curvature of third antisymmetric mode.

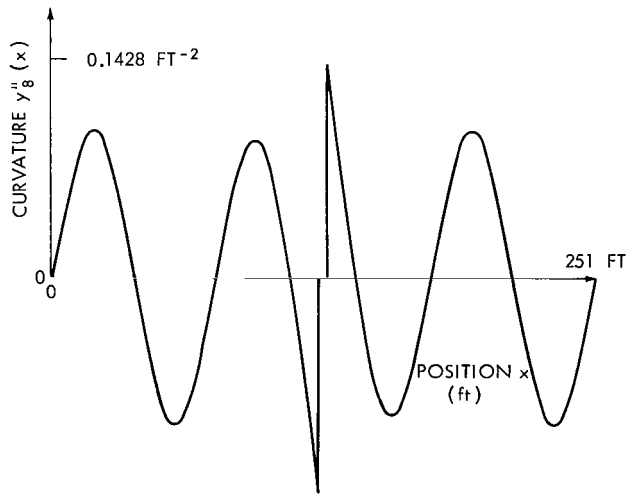

Figure 27—Curvature of fourth antisymmetric mode.

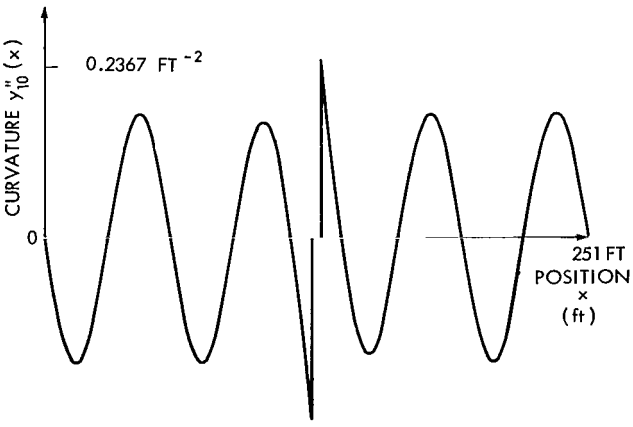

Figure 28—Curvature of fifth antisymmetric mode.

From Figures 9 through 28, the following observations can be made concerning the possible effects of vibrational motion on the ATS-D system:

1. Figures 9 through 18 show that the satellite body and tip weights will be essentially pinned in inertial space for all modes of vibration except the first symmetric mode.

2. Figures 14, 15, and 16 show that if any one of the first three antisymmetric modes of vibration are excited, the rotational inertia of the satellite body is not large enough to prevent significant rotational motion of the body about the center of mass.

3. For all modes of oscillation except the first antisymmetric mode, the peak curvature and hence the peak bending moment will exist at the boom's root. For the first antisymmetric mode (see Figure 24) the point of peak curvature will occur at a point 45 feet from the root. The curvature at this point will be about 1.5 times the curvature at the root.

The object of this example is to determine whether the viscoelastic damping of the boom material itself can prevent the bending moment at any point along the boom from exceeding its critical buckling moment when the system is excited at a resonant frequency.

This may be done by directly comparing the critical buckling moment and peak bending moment of the system for each excitation frequency under study. We can avoid evaluating the complete expression defining the peak bending moment,

$$\max_x \max_t EI\, Y''(x, t) = \max_x \max_t EI \sum_{n=1}^{\infty} a_n(t)\, y_n''(x) , \tag{6.9}$$

by using the following fact: when the system is excited by the triangular wave whose period equals one of the natural periods of the system, the major contribution to the resultant bending moment at any point is associated with the particular mode excited at resonance.

Thus, when the excitation period t_2 defined in Equation 6.2 is given by

$$t_2 = \frac{2\pi}{\omega_n} \tag{6.10}$$

and the rise time t_1 is given by

$$t_1 = \frac{t_2}{3} = \frac{2\pi}{3\omega_n} , \tag{6.11}$$

the peak bending moment is approximated by the expression

$$\max_x \max_t EI\, Y''(x, t) \doteq \max_x \max_t EI\, a_n(t)\, y_n''(x) . \tag{6.12}$$

It will be recalled that for all modes of vibration except the first antisymmetric ($n = 2$) the peak curvature is at the boom root; i.e., at $x = L \pm R$, and that

$$|y_n''(L+R)| = |y_n''(L-R)| . \tag{6.13}$$

Therefore, by applying this fact the maximization on x called for in Equation 6.12 can be performed. This leads to the expression

$$\max_x \max_t EI\, Y''(x,t) \doteq \begin{cases} EI \max_t a_n(t)\, y_n''(L+R), & \text{for } n \neq 2, \\ 1.5\, EI \max_t a_n(t)\, y_n''(L+R), & \text{for } n = 2, \end{cases} \tag{6.14}$$

where, for $n = 2$, the peak curvature is 1.5 times the curvature at the root. The maximization on t called for in Equation 6.14 can be performed by directly substituting Equations 6.3 through 6.8 in Equation 4.22 and computing the maximum value of $a_n(t)_{ST}$ in the interval $0 \leq t \leq t_2$.

The points marked on Figure 29 show what the contribution to the peak bending moment at the boom root would be for each mode if it were excited at its natural period. That is, for the excitation frequency

$$\omega_n = \frac{2\pi}{t_2} \tag{6.15}$$

shown on the horizontal scale, the magnitude of

$$\max_x \max_t EI\, a_n(t)\, y_n''(x)$$

can be ascertained from the vertical scale.

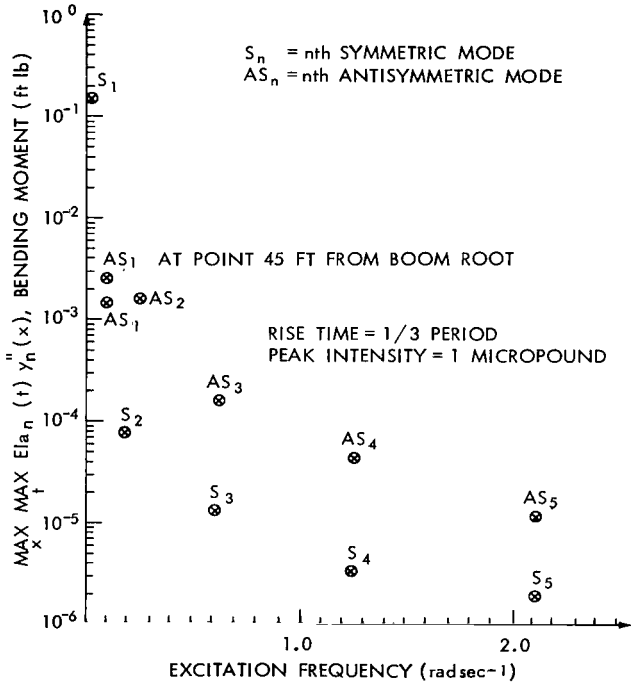

Figure 29—Peak bending moment contribution at boom root from each mode for a triangular forcing function having a frequency equal to natural frequency.

Thus, even if the damping ratio were as low as 10^{-4} and the microthruster did excite a resonant frequency, the critical buckling moment—which is about one ft-lb—would not be exceeded.

SUMMARY

The equations developed herein may be applied to any satellite having long elastic members that can be modeled as a symmetric double-beam system, as shown in Figure 1. The following is

a summary of the equations and the conclusions that can be drawn by a close examination of them and the figures.

1. Because of the system's symmetry, the normalized modes of vibration can be separated into two groups: symmetric and antisymmetric, respectively, about the system's axis of symmetry. Equations 5.1 and 5.2 are the frequency equations of the symmetric and antisymmetric modes, respectively.

2. The frequency equations are written in terms of the dimensionless parameters:

(a) W_T/W_B = ratio of tip to beam weight

(b) R/L_0 = ratio of satellite body radius to beam length

(c) W_s/W_B = ratio of satellite body to beam weight

(d) I_s/I_B = ratio of satellite body to beam inertia

The natural frequencies of the system may be determined with slide-rule accuracy by simply defining the above parameters and interpolating between the appropriate curves on Figures 3, 6 and 7.

3. The following conclusions may be drawn from Equations 5.1 and 5.2 and the corresponding figures.

(a) For $W_s/W_B > 100$ and $W_T/W_B < 20$, the frequency associated with the first symmetric mode of vibration is approximately that of a clamped beam with tip weight.

(b) For $I_s/I_B > 0.1$, $0 < R/L_0 \leq 0.1$ and $0 \leq W_T/W_B \leq \infty$, the frequency associated with the first antisymmetric mode of vibration is approximately independent of R/L_0.

(c) For $I_s/I_B < 0.1$, $0.05 < R/L_0 < 0.1$, and $0 \leq W_T/W_B < \infty$, the quantity R/L_0 becomes a significant parameter in the prediction of the first antisymmetric modal frequency.

(d) For $I_s/I_B > 250$ and $W_T/W_B < 30$, the frequency associated with the first antisymmetric mode of vibration is approximately that of a clamped beam with tip weight.

(e) For $I_s/I_B < 5$ and $W_T/W_B > 10$, the frequency associated with the first antisymmetric mode of vibration is approximately that of a similar system having its tips hinged in inertial space.

(f) For $W_T/W_B > 3$, all higher symmetric and antisymmetric modes of vibration can be approximated by a similar system having its tips hinged in inertial space.

4. The equations defining the symmetric and antisymmetric mode shapes are developed in terms of dimensionless parameters and are given by Equations 3.1 and 3.2.

5. The equations defining both the transient and the steady-state response of the system in terms of its normal modes of vibration are derived for an arbitrary force distribution of periodic intensity. These Equations are 4.17, 4.18, and 4.22.

Goddard Space Flight Center
National Aeronautics and Space Administration
Greenbelt, Maryland, February 5, 1968
630-12-02-01-51

REFERENCES

1. Bishop, R. E. D., Gladwell, G. M. L., and Michaelson, S., "The Matrix Analysis of Vibration," Cambridge Univ. Press, 1965.

2. Churchill, R. V., "Operational Mathematics," New York: McGraw Hill, 1958.

3. Hurty, W. C., and Rubinstein, M. F., "Dynamics of Structures," Englewood Cliffs, N. J.: Prentice Hall, 1964.

4. Predmore, R. E., Staugaitis, C. L, and Jellison, J. E., "Damping Behaviour of DeHavilland Stem Booms," NASA TN D-3996, 1967.

Appendix A

Symbol List

$a_n(t)$ time-dependent generalized displacement coordinate associated with the nth mode, ft.

b_m mth Fourier cosine coefficient.

C_1, C_2, C_3, C_4 constants of integration.

d_m mth Fourier sine coefficient.

$EI(x)$ bending stiffness at x, lb ft^2.

EI bending stiffness along length of elastic beam, lb ft^2.

$F(x, t)$ force distribution at (x, t), lb ft^{-1}.

$F_1(x, t)$ $F_1(x)f(t)$ force distribution of periodic intensity that is symmetric about the system's axis of symmetry and excites only the symmetric modes of vibration, lb ft^{-1}.

$F_2(x, t)$ $F_2(x)f(t)$ force distribution of periodic intensity that is antisymmetric about the system's axis of symmetry and excites only the antisymmetric modes of vibration, lb ft^{-1}.

g acceleration of gravity, ft sec^{-2}.

I_B mass moment of inertia of a beam of length $2L_0$ about an axis normal to the length and passing through its centroid, slugs ft^2.

I_s mass moment of inertia of rigid satellite body (without beams and tip weights) about the axis through the center of mass and normal to the plane of vibration, slugs ft^2.

$2L$ length of entire system, ft.

L_0 length of one beam, ft.

M_T total mass of entire system, slugs.

m, n integers 0, 1, 2 · · ·

$2R$ total length of rigid satellite body, ft.

$2R^*$ normalized length of rigid satellite body.

t	time, sec.
t_1	rise time of triangular wave, sec.
t_2	period of triangular wave, sec.
W_B	weight of single beam without tip weight.
W_T	tip weight, lb.
W_s	weight of rigid satellite body (without beams and tip weights), lb.
W_s^*	effective inertia weight of satellite body, lb.
x	position coordinate measured positive from the beam tip, ft.
$y_n(x)$	nth normalized mode of the undamped unforced equations of motion of the entire system.
$y_n^*(z)$	nth mode of the undamped unforced equation of motion of one beam, used to construct $y_n(x)$.
$Y(x, t)$	transverse displacement at (x, t), ft.
z	position coordinate defined over flexible portion of one beam, ft.
$\beta(x)$	viscous damping coefficient at x, lb sec ft^{-2}.
β	viscous damping coefficient of the beams alone, lb sec ft^2.
$\delta(x)$	Dirac Delta function.
$\delta_{n, m}$	Kronecker Delta function.
$\rho(x)$	mass distribution of the satellite beam system at x, slugs ft^{-1}.
ρ	mass distribution along the beam, slugs ft^{-1}.
ζ_n	damping ratio associated with the nth mode.
ζ	damping ratio measured experimentally.
λ_n	nth eigenvalue of the defined eigenvalue problem.
ω_n	nth natural frequency of system.
θ	frequency of applied force distribution.
ν_n	inverse of the time constant associated with the nth mode of vibration.
Ω_n	damped natural frequency of the th mode of vibration.

NATIONAL AERONAUTICS AND SPACE ADMINISTRATION
WASHINGTON, D.C. 20546

OFFICIAL BUSINESS

FIRST CLASS MAIL

POSTAGE AND FEES PAID
NATIONAL AERONAUTICS AND
SPACE ADMINISTRATION

POSTMASTER: If Undeliverable (Section 158 Postal Manual) Do Not Return

"The aeronautical and space activities of the United States shall be conducted so as to contribute . . . to the expansion of human knowledge of phenomena in the atmosphere and space. The Administration shall provide for the widest practicable and appropriate dissemination of information concerning its activities and the results thereof."

— NATIONAL AERONAUTICS AND SPACE ACT OF 1958

NASA SCIENTIFIC AND TECHNICAL PUBLICATIONS

TECHNICAL REPORTS: Scientific and technical information considered important, complete, and a lasting contribution to existing knowledge.

TECHNICAL NOTES: Information less broad in scope but nevertheless of importance as a contribution to existing knowledge.

TECHNICAL MEMORANDUMS: Information receiving limited distribution because of preliminary data, security classification, or other reasons.

CONTRACTOR REPORTS: Scientific and technical information generated under a NASA contract or grant and considered an important contribution to existing knowledge.

TECHNICAL TRANSLATIONS: Information published in a foreign language considered to merit NASA distribution in English.

SPECIAL PUBLICATIONS: Information derived from or of value to NASA activities. Publications include conference proceedings, monographs, data compilations, handbooks, sourcebooks, and special bibliographies.

TECHNOLOGY UTILIZATION PUBLICATIONS: Information on technology used by NASA that may be of particular interest in commercial and other non-aerospace applications. Publications include Tech Briefs, Technology Utilization Reports and Notes, and Technology Surveys.

Details on the availability of these publications may be obtained from:

SCIENTIFIC AND TECHNICAL INFORMATION DIVISION

NATIONAL AERONAUTICS AND SPACE ADMINISTRATION

Washington, D.C. 20546